

The nonconforming virtual element method with curved edges

Lourenco Beirão Da Veiga^{*†}, Yi Liu^{*‡}, Lorenzo Mascotto^{*†§}, Alessandro Russo^{*†}

Abstract

We introduce a nonconforming virtual element method for the Poisson equation on domains with curved boundary and internal interfaces. We prove arbitrary order optimal convergence in the energy and L^2 norms, and validate the theoretical results with numerical experiments. Compared to existing nodal virtual elements on curved domains, the proposed scheme has the advantage that it can be designed in any dimension.

AMS subject classification: 65N15; 65N30.

Keywords: nonconforming virtual element method; polytopal mesh; curved domain; optimal convergence.

1 Introduction

Partial differential equations are often posed on domains with curved boundaries and internal interfaces. The geometric error between a curved interface/boundary and a corresponding “flat” approximation affects the accuracy of the standard finite element method, leading to a loss of convergence for higher-order elements [32, 33]. This phenomenon has been addressed in many different ways in the literature, the most classical being to employ isoparametric finite elements [26, 28], which require a polynomial approximation of the curved boundary and a careful choice of the isoparametric nodes; another notable approach, which applies to CAD domains, is that of the Isogeometric Analysis [21].

Both issues can be avoided employing curved virtual elements [10]. The virtual element method [5, 7] was designed a decade ago as a generalization of the finite element method to a Galerkin method based on polytopal meshes. Basis functions are defined as solutions to local partial differential problems with polynomial data. An explicit representation of the basis functions is not required; rather, the scheme is designed only based on a suitable choice of the degrees of freedom.

In [10], test and trial virtual element functions are defined (in 2D) so as their restrictions on curved edges are mapped polynomials. Other variants were developed later. In [8], again focusing on the 2D case only, virtual element functions over curved edges are restrictions of polynomials. In [11], a boundary correction technique tracing back to the pioneering work [13] was generalized to the virtual element setting; here, normal-directional Taylor expansions are used to correct function values on the boundary. The gospel of [10] has been applied to the approximation of solutions to the wave equation in [23]. Mixed virtual elements on curved domains are analyzed in two and three dimensions in [22, 24].

Other polytopal element method have been designed for curved domains. Amongst them, we recall the extended hybridizable discontinuous Galerkin method [27]; the unfitted hybrid high-order method [17, 16]; the hybrid high-order method for the Poisson [12, 34] and (singularly perturbed) fourth order problems [25]; the Trefftz-based finite element method [2].

^{*}Dipartimento di Matematica e Applicazioni, Università degli Studi di Milano-Bicocca, 20125 Milano, Italy, lourenco.beirao@unimib.it, yi.liu@unimib.it, lorenzo.mascotto@unimib.it, alessandro.russo@unimib.it

[†]IMATI-CNR, 27100, Pavia, Italy

[‡]School of Mathematical Sciences, Nanjing Normal University, Nanjing 210023, China, 200901005@njnu.edu.cn

[§]Fakultät für Mathematik, Universität Wien, 1090 Vienna, Austria

In this paper, we focus on the Poisson problem, design a nonconforming virtual element method on curved domains and with internal curved interfaces, prove arbitrary order optimal convergence estimates in the energy and L^2 norms, and validate the theoretical results with numerical results.

The proposed scheme is a generalization of the standard nonconforming virtual element method to the case of curved boundaries and internal interfaces. Indeed, when the curved boundaries happen to be straight, the proposed virtual space boils down to that in [3]. Compared to its conforming nodal version [10], in principle the nonconforming scheme can be designed and analyzed in any dimension at once.

The proposed method is based on the computation of a novel Ritz-Galerkin operator that, due to computability reasons, is different from the standard H^1 projection operator typically employed in virtual elements. A noteworthy challenge of the forthcoming analysis resides in developing optimal approximation estimates for such a Ritz-Galerkin operator; this result is interesting per se and could be borrowed also by other methods handling curved boundaries/interfaces.

Even though the standard nonconforming virtual element can be algebraically equivalent to the hybrid high-order method [20] for a particular choice of the stabilization, the method presented in this paper differs from the hybrid-high order methods on curved domains available in the literature.

Preliminary notation. We denote the usual Sobolev space of order m , $m \geq 0$, on an open bounded Lipschitz domain D in \mathbb{R}^d , $d \in \mathbb{N}$, by $H^m(D)$. We endow it with the inner-product $(\cdot, \cdot)_{m,D}$, the norm $\|\cdot\|_{m,D}$, and the seminorm $|\cdot|_{m,D}$. Let $H_0^1(D)$ the subspace of $H^1(D)$ of functions with zero trace over the boundary ∂D of D . When $m = 0$, the space $H^0(D)$ is the space $L^2(D)$ of square integrable functions over D . In this case, $(\cdot, \cdot)_{0,D} = (\cdot, \cdot)_D$ denotes the standard L^2 inner-product. Sobolev spaces of negative order can be defined by duality. The notation $\langle \cdot, \cdot \rangle$ stands for the duality pairing $H^{-\frac{1}{2}} - H^{\frac{1}{2}}$ on a given domain.

Further, we introduce the Sobolev spaces $W^{m,\infty}(D)$, $m \in \mathbb{N}$, of functions having weak derivatives up to order m , which are bounded almost everywhere in D . The case $m = 0$ coincides with the usual space $L^\infty(D)$; the spaces of noninteger order $m \geq 0$, $m \notin \mathbb{N}$, are constructed, e.g., by interpolation theory. The corresponding norm and seminorm are $\|\cdot\|_{W^{m,\infty}(D)}$ and $|\cdot|_{W^{m,\infty}(D)}$.

Model problem. Let $\Omega \subset \mathbb{R}^d$, $d = 2, 3$, be a Lipschitz domain with (possibly) curved boundary $\partial\Omega$. Given f in $L^2(\Omega)$ and g in $H^{\frac{1}{2}}(\partial\Omega)$, we consider the following Poisson problem: Find u such that

$$\begin{cases} -\Delta u = f & \text{in } \Omega, \\ u = g & \text{on } \partial\Omega. \end{cases} \quad (1.1)$$

Introduce $V_g = \{u \in H^1(\Omega) : u|_{\partial\Omega} = g\}$, $V := H_0^1(\Omega)$, and the bilinear form

$$a(u, v) := \int_{\Omega} \nabla u \cdot \nabla v \, d\Omega \quad \forall u, v \in H^1(\Omega).$$

A variational formulation of (1.1) reads as follows:

$$\begin{cases} \text{Find } u \in V_g \text{ such that} \\ a(u, v) = (f, v)_{0,\Omega} \quad \forall v \in V. \end{cases} \quad (1.2)$$

We assume that the boundary $\partial\Omega$ is the union a finite number of smooth curved edges/faces $\{\Gamma_i\}_{i=1,\dots,N}$, i.e.,

$$\bigcup_{i=1}^N \Gamma_i = \partial\Omega.$$

Each Γ_i is of class \mathcal{C}^η , for an integer $\eta \geq 1$, which will fixed in Assumption 5.1 below: if $d = 2$, there exists a given regular and invertible \mathcal{C}^η -parametrization $\gamma_i : I_i \rightarrow \Gamma_i$ for $i = 1, \dots, N$, where

$I_i := [a_i, b_i] \subset \mathbb{R}$ is a closed interval; if $d = 3$, there exists a given regular and invertible \mathcal{C}^η -parametrization $\gamma_i : F_i \rightarrow \Gamma_i$ for $i = 1, \dots, N$, where F_i is a straight polygon. The smoothness parameter η depends on the order of the numerical scheme and will be specified later.

Since all the Γ_i can be treated analogously in the forthcoming analysis, we drop the index i and assume that $\partial\Omega$ contains only one curved face Γ . To further simplify the presentation, we focus on the two dimensional case and postpone the discussion of the three dimensional case to Section 7 below. We further assume that $\gamma : [0, 1] \rightarrow \Gamma$.

Remark 1.1. *The forthcoming analysis can be extended to the case of internal interfaces (and jumping coefficients) with minor modifications. To simplify the presentation, we stick to the case of Γ being a curved boundary face; however, we shall present numerical experiments for jumping coefficients across internal curved interfaces.*

Structure of the paper. In Section 2, we introduce regular polygonal meshes, and broken and nonconforming polynomial and Sobolev spaces. In Section 3, we design a novel nonconforming virtual element method for curved domain; show its well posedness; discuss its lack of polynomial consistency. In Sections 4 and 5, we prove stability and interpolation properties of the new virtual element functions. Section 6 is devoted to the proof of the rate of convergence in the H^1 and L^2 norms. Details on the 3D version of the method are discussed in Section 7. In Section 8, we present numerical experiments that verify the theory established the previous sections.

2 Meshes and broken spaces

In this section, we introduce regular polygonal meshes with whom we associate broken polynomial and Sobolev spaces, and nonconforming polynomial spaces.

2.1 Mesh assumptions

Let $\{\mathcal{T}_h\}$ be a sequence of partitions of Ω into polygons, possibly with curved edges along the curved boundary. We denote the diameter of each element K by h_K and the mesh size function of \mathcal{T}_h by $h := \max_{K \in \mathcal{T}_h} h_K$. Let \mathcal{E}_h be the set of edges in \mathcal{T}_h . We denote the size of any edge e by h_e , where the size of a (possibly curved) edge is the distance between its two endpoints; see Remark 2.1 below. Let \mathcal{E}_h^I and \mathcal{E}_h^B be the sets of all interior and boundary edges in \mathcal{T}_h with $\mathcal{E}_{h,c}$ and $\mathcal{E}_{h,s}$ denoting the sets of curved and straight edges in \mathcal{T}_h , respectively.

For each element $K \in \mathcal{T}_h$, we denote the sets of its edges by \mathcal{E}^K , which we split into straight \mathcal{E}_s^K and curved edges \mathcal{E}_c^K , respectively. We denote the set of elements containing at least one edge in \mathcal{E}_h^B by \mathcal{T}_h^B ; an element K in \mathcal{T}_h^B may contain more than one edge in \mathcal{E}_h^B . With each element K , we associate the outward unit normal vector \mathbf{n}_K ; with each edge e , we associate a unit normal vector \mathbf{n}_e out of the available two.

Henceforth, we demand the following regularity assumptions on the sequence $\{\mathcal{T}_h\}$: there exists a positive constant ρ such that

- (G1) each element K is star-shaped with respect to a ball of radius larger than or equal to ρh_K ;
- (G2) for each element K and any of its (possibly curved) edges e , h_e is larger than or equal to ρh_K .

Assumptions (G1)–(G2) imply that each element has a uniformly bounded number of edges.

We introduce a parametrization of the edges:

- for any straight edge e with endpoints \mathbf{x}_e^1 and \mathbf{x}_e^2 , we introduce the parametrization $\gamma_e(t) = \frac{t}{h_e}(\mathbf{x}_e^2 - \mathbf{x}_e^1) + \mathbf{x}_e^1$;
- for any curved edge e , we introduce the parametrization $\gamma_e : I_e \subset I := [0, 1] \rightarrow e$ as the restriction of the global parametrization $\gamma : I \rightarrow \Gamma$ to the interval I_e .

Remark 2.1. Let the length of a curved edge $\ell_e = \int_{I_e} \|\gamma'(t)\| dt$. Since γ and γ^{-1} are fixed once and for all, and are of class $W^{1,\infty}$, the quantity h_e introduced above is comparable with ℓ_e . Therefore in the following we shall simply refer to both quantities as “length”.

We shall write $x \lesssim y$ and $x \gtrsim y$ instead of $x \leq Cy$ and $x \geq Cy$, respectively, for a positive constant C independent of \mathcal{T}_h . Moreover, $x \approx y$ stands for $x \lesssim b$ and $b \lesssim a$ at once. The involved constants will be written explicitly only when necessary.

The validity of **(G1)**–**(G2)** guarantees that the constants in the forthcoming trace and inverse inequalities are uniformly bounded.

2.2 Broken and nonconforming spaces

Let $\mathbb{P}_n(K)$, $n \in \mathbb{N}$, be the space of polynomials of maximum degree n over each element K ; we use the convention $\mathbb{P}_{-1}(K) = \{0\}$. Given \mathbf{x}_K the centroid of K , we introduce a basis for the space $\mathbb{P}_n(K)$ given by the set of scaled and shifted monomials

$$\mathcal{M}_n(K) = \left\{ \left(\frac{\mathbf{x} - \mathbf{x}_K}{h_K} \right)^\alpha \mid \forall \alpha \in \mathbb{N}^2, |\alpha| \leq n, \forall \mathbf{x} \in K \right\}.$$

Here, α denotes a multi-index $\alpha = (\alpha_1, \alpha_2)$.

Similarly, let $\mathbb{P}_n(I_e)$, $n \in \mathbb{N}$, be the space of polynomials of maximum degree n over the interval I_e . Given x_{I_e} and h_{I_e} the midpoint and length of I_e , we introduce a basis for the space $\mathbb{P}_n(I_e)$ given by the set of scaled and shifted monomials

$$\mathcal{M}_n(I_e) = \left\{ \left(\frac{x - x_{I_e}}{h_{I_e}} \right)^\alpha \mid \forall \alpha \in \mathbb{N}, \alpha \leq n, \forall x \in I_e \right\}.$$

Recalling that $\gamma_e : I_e \subset I \rightarrow e$ denotes the parametrization of the edge e , we consider the following mapped polynomial space and scaled monomial set:

$$\tilde{\mathbb{P}}_n(e) = \{\tilde{q} = q \circ \gamma_e^{-1} : q \in \mathbb{P}_n(I_e)\}, \quad \tilde{\mathcal{M}}_n(e) = \{\tilde{m} = m \circ \gamma_e^{-1} : m \in \mathcal{M}_n(I_e)\}.$$

If e is straight, then $\tilde{\mathbb{P}}_n(e)$ and $\tilde{\mathcal{M}}_n(e)$ boil down to a standard polynomial space and scaled monomial set, respectively. For any $s > 0$, we introduce the broken Sobolev space over a mesh \mathcal{T}_h as

$$H^s(\mathcal{T}_h) := \{v \in L^2(\Omega) : v|_K \in H^s(K) \quad \forall K \in \mathcal{T}_h\},$$

and equip it with the broken norm and seminorm

$$\|v\|_{s,h}^2 := \sum_{K \in \mathcal{T}_h} \|v\|_{s,K}^2, \quad |v|_{s,h}^2 := \sum_{K \in \mathcal{T}_h} |v|_{s,K}^2.$$

We define the jump across the edge e of any v in $H^1(\mathcal{T}_h)$ as

$$[[v]] := \begin{cases} v|_{K^+ \mathbf{n}_{K^+}} + v|_{K^- \mathbf{n}_{K^-}} & \text{if } e \in \mathcal{E}_h^I, e \subset \partial K^+ \cap \partial K^- \text{ for given } K^+, K^- \in \mathcal{T}_h \\ v \mathbf{n}_e & \text{if } e \in \mathcal{E}_h^B, e \subset K \text{ for a given } K \in \mathcal{T}_h. \end{cases}$$

The nonconforming Sobolev space of order k over \mathcal{T}_h is given as follows:

$$H^{1,nc}(\mathcal{T}_h, k) := \left\{ v \in H^1(\mathcal{T}_h) \mid \int_e [[v]] \cdot \mathbf{n}_e \, q \, ds = 0, \forall q \in \tilde{\mathbb{P}}_{k-1}(e), \forall e \in \mathcal{E}_h \right\}.$$

In the straight edges case, this space coincides with the standard nonconforming Sobolev space in [3].

3 The nonconforming virtual element method on curved polygons

In this section, we introduce the nonconforming virtual element method for the approximation of solutions to (1.2). In Section 3.1, we introduce the local and global virtual element spaces and endow them with suitable sets of degrees of freedom (DoFs). In Section 3.2, we discretize the bilinear form by means of computable polynomial projectors and stabilizing bilinear forms. With this at hand, we introduce the method in Section 3.3.

3.1 Nonconforming virtual element spaces

We define a local virtual element space of order k in \mathbb{N} on the (possibly curved) element K :

$$V_h(K) := \left\{ v_h \in H^1(K) \mid \Delta v_h \in \mathbb{P}_{k-2}(K), \mathbf{n}_K \cdot \nabla v_h \in \widetilde{\mathbb{P}}_{k-1}(e) \forall e \in \mathcal{E}^K \right\}. \quad (3.1)$$

We have that $\mathbb{P}_n(K)|_e = \widetilde{\mathbb{P}}_n(e)$ if e is a straight edge; instead, if e is a curved edge, $\mathbb{P}_0(K)|_e \subset \widetilde{\mathbb{P}}_n(e)$ but in general, $\mathbb{P}_n(K)|_e \not\subset \widetilde{\mathbb{P}}_n(e)$. This implies that on curved elements the space $V_h(K)$ contains constant functions but not the space $\mathbb{P}_k(K)$.

We can define the following sets of degrees of freedom for the space $V_h(K)$.

- on each edge e of K , the moments

$$\mathbf{D}_e^i(v_h) = |e|^{-1} \int_e v_h \tilde{m}_i \, ds \quad \forall \tilde{m}_i \in \widetilde{\mathcal{M}}_{k-1}(e); \quad (3.2)$$

- the bulk moments

$$\mathbf{D}_K^j(v_h) = |K|^{-1} \int_K v_h m_j \, dK \quad \forall m_j \in \mathcal{M}_{k-2}(K). \quad (3.3)$$

In Figure 3.1, we give a graphic representation for such linear functionals in the case $k = 2$.

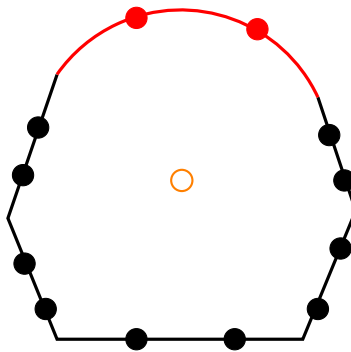


Figure 3.1: Representation of the DoFs for $k = 2$. The edge moments (3.2) are the black balls (for straight edges) and red balls (for curved edges); the bulk moments (3.3) are the internal orange circles.

The following result generalizes [3, Lemma 3.1] to the case of curved elements.

Lemma 3.1. *The sets of linear functionals (3.2) and (3.3) are a set of unisolvent DoFs for the space $V_h(K)$.*

Proof. The number of linear functionals in (3.2) and (3.3) equals the dimension of the space $V_h(K)$. So, we only have to prove the unisolvence. Let v_h in $V_h(K)$ be such that

$$\mathbf{D}_e^i(v_h) = 0 \quad \forall e \in \mathcal{E}^K \quad \text{and} \quad \mathbf{D}_K^j(v_h) = 0 \quad \forall i = 1, \dots, k; \quad j = 1, \dots, k(k-1)/2. \quad (3.4)$$

Then, it suffices to prove $v_h = 0$. To this aim, we integrate by parts, use (3.4), and obtain

$$\int_K |\nabla v_h|^2 \, dK = \int_K -\Delta v_h v_h \, dK + \sum_{e \in \mathcal{E}^K} \int_e \mathbf{n}_K \cdot \nabla v_h v_h \, ds = 0.$$

We deduce $\nabla v_h = 0$ in K , whence v_h is constant. Thanks to (3.4), v_h has zero average over each edge. The assertion follows. \square

The global nonconforming virtual element space is constructed by a standard coupling of the interface degrees of freedom (3.2):

$$V_h(\mathcal{T}_h) := \{v_h \in H^{1,nc}(\mathcal{T}_h, k) \mid v_h|_K \in V_h(K) \, \forall K \in \mathcal{T}_h\}. \quad (3.5)$$

Further, we define nonconforming virtual element spaces with weakly imposed boundary conditions: if g is in $L^1(\partial\Omega)$,

$$V_h^g(\mathcal{T}_h) := \left\{ v_h \in V_h(\mathcal{T}_h) \mid \int_e (v_h - g) \tilde{q}_{k-1} = 0 \quad \forall \tilde{q}_{k-1} \in \tilde{\mathbb{P}}_{k-1}(e), \quad e \in \mathcal{E}_h^B \right\}. \quad (3.6)$$

The above spaces and degrees of freedom are a generalization to curved elements of their straight counterparts in [3]. Interpolation estimates are derived in Section 5 below.

Remark 3.2. *The enhanced version of the space $V_h(K)$ [1] involves a modification of the space inside the element and not on the (curved) edges. Therefore, designing an enhanced version of the local spaces in (3.1) is straightforward by combining the tools in [1] with the techniques presented here.*

3.2 Polynomial projectors and discrete bilinear forms

Here, we introduce projections onto polynomial spaces, stabilizing bilinear forms, and a discrete bilinear form.

Projections onto polynomial spaces. On each element K , we introduce projection operators onto polynomial spaces of maximum degree n in \mathbb{N} :

- the (possibly curved) edge L^2 projection $\tilde{\Pi}_n^{0,e} : L^2(e) \rightarrow \tilde{\mathbb{P}}_n(e)$ given by

$$\int_e \tilde{q}_n (v - \tilde{\Pi}_n^{0,e} v) \, ds = 0 \quad \forall \tilde{q}_n \in \tilde{\mathbb{P}}_n(e); \quad (3.7)$$

- the Ritz-Galerkin projection $\tilde{\Pi}_n^{\nabla,K} : H^1(K) \rightarrow \mathbb{P}_n(K)$ satisfying, for all q_n in $\mathbb{P}_n(K)$,

$$\begin{aligned} \int_K \nabla q_n \cdot \nabla \tilde{\Pi}_n^{\nabla,K} v \, dK &= - \int_K \Delta q_n v \, dK + \sum_{e \in \mathcal{E}_h^K} \int_e \tilde{\Pi}_{n-1}^{0,e} (\mathbf{n}_K \cdot \nabla q_n) v \, ds \\ &= - \int_K \Delta q_n v \, dK + \sum_{e \in \mathcal{E}_{h,s}^K} \int_e (\mathbf{n}_K \cdot \nabla q_n) v \, ds + \sum_{e \in \mathcal{E}_{h,c}^K} \int_e \tilde{\Pi}_{n-1}^{0,e} (\mathbf{n}_K \cdot \nabla q_n) v \, ds, \end{aligned} \quad (3.8)$$

together with

$$\begin{cases} \int_{\partial K} (v - \tilde{\Pi}_n^{\nabla,K} v) \, ds = 0 & \text{if } n = 1, \\ \int_K (v - \tilde{\Pi}_n^{\nabla,K} v) \, dK = 0 & \text{if } n \geq 2; \end{cases} \quad (3.9)$$

- the L^2 projection $\Pi_n^{0,K} : L^2(K) \rightarrow \mathbb{P}_n(K)$ given by

$$\int_K q_n(v - \Pi_n^{0,K}v) \, dK = 0 \quad \forall q_n \in \mathbb{P}_n(K). \quad (3.10)$$

Remark 3.3. *If all the edges of an element K are straight, then $\tilde{\Pi}_k^{\nabla,K} q_k = q_k$ for all q_k in $\mathbb{P}_k(K)$ and $\tilde{\Pi}_k^{\nabla,K}$ boils down to the standard VEM operator $\Pi_k^{\nabla,K}$ [5]. Instead, if at least one edge of K is curved, then $\tilde{\Pi}_k^{\nabla,K} q_k \neq q_k$ unless $k = 0$. This fact is the reason of the lack of polynomial consistency of the method on curved elements.*

Next, we show that the three projectors above are computable by means of the DoFs.

Proposition 3.4. *Given the DoFs (3.2)–(3.3) of a given v_h in $V_h(K)$, we can compute $\tilde{\Pi}_{k-1}^{0,e} v_h|_e$, $\Pi_{k-2}^{0,K} v_h$, and $\tilde{\Pi}_k^{\nabla,K} v_h$, where the three operators are defined in (3.7), (3.8)–(3.9), and (3.10), respectively.*

Proof. The computability of $\tilde{\Pi}_{k-1}^{0,e} v_h|_e$ and $\Pi_{k-2}^{0,K}$ follows immediately from the edge and bulk DoFs, respectively. As for $\tilde{\Pi}_k^{\nabla,K} v_h$, since the average condition (3.9) is obviously computable, it suffices to show the computability of the right hand side of (3.8). The first term on the right-hand side is computable from (3.3); the second and third terms are computable from (3.2). \square

Remark 3.5. *Differently from the standard nonconforming virtual element framework [3], we do not use an H^1 projection, but rather the Ritz-Galerkin projection $\tilde{\Pi}_k^{\nabla,K}$ in (3.8)–(3.9). The reason is that the definition of the local space and the choice of the DoFs would not allow us to compute the standard H^1 projection from the degrees of freedom, due to the noncomputability of $\int_e (\mathbf{n}_K \cdot \nabla q_n) v_h$ on curved edges.*

A discrete bilinear form. We define a discrete local bilinear form $a_h^K(\cdot, \cdot) : V_h(K) \times V_h(K) \rightarrow \mathbb{R}$ on each element K as follows:

$$a_h^K(u_h, v_h) = a^K(\tilde{\Pi}_k^{\nabla,K} u_h, \tilde{\Pi}_k^{\nabla,K} v_h) + S^K((I - \tilde{\Pi}_k^{\nabla,K})u_h, (I - \tilde{\Pi}_k^{\nabla,K})v_h) \quad \forall u_h, v_h \in V_h(K).$$

Above, $S^K(\cdot, \cdot) : V_h(K) \times V_h(K) \rightarrow \mathbb{R}$ is a bilinear form that satisfies two properties: it is computable via the local set of DoFs over K ; it satisfies the stability bounds

$$|v_h|_{1,K}^2 \lesssim S^K(v_h, v_h) \lesssim |v_h|_{1,K}^2 \quad \forall v_h \in V_h(K) \cap \ker(\tilde{\Pi}_k^{\nabla,K}). \quad (3.11)$$

Denoting by $\{\mathbf{D}^l\}_{l=1}^{N_{\text{dof}}(K)}$ the set of all degrees of freedom of $V_h(K)$, a possible stabilization satisfying (3.11) is

$$S^K(u_h, v_h) = \sum_{l=1}^{N_{\text{dof}}(K)} \mathbf{D}^l(u_h) \mathbf{D}^l(v_h),$$

which can be rewritten in terms of boundary and bulk contributions as

$$S^K(u_h, v_h) = \sum_{e \in \mathcal{E}^K} \sum_{i=1}^k \mathbf{D}_e^i(u_h) \mathbf{D}_e^i(v_h) + \sum_{j=1}^{k(k-1)/2} \mathbf{D}_K^j(u_h) \mathbf{D}_K^j(v_h). \quad (3.12)$$

We postpone to Section 4 below the analysis of such a stabilizing term. Of course, other stabilizations satisfying the computability and stability properties can be defined; we stick to the choice in (3.12) since it is the most popular in the virtual element community.

Remark 3.6. *The bilinear form $a_h^K(\cdot, \cdot)$ does not satisfy the usual consistency property of the virtual element method [3, 5] when K is a curved polygon. The reason is the use of a polynomial projection that is not the usual H^1 projection; see Remark 3.3 for further details.*

Finally, we introduce a global discrete bilinear form $a_h(\cdot, \cdot) : V_h \times V_h \rightarrow \mathbb{R}$ defined as

$$a_h(u_h, v_h) = \sum_{K \in \mathcal{T}_h} a_h^K(u_h, v_h) \quad \forall u_h, v_h \in V_h. \quad (3.13)$$

The discrete right-hand side. Here, we construct a computable discretization of the right-hand side $(f, v_h)_{0,\Omega}$ in (1.2). For $k \geq 2$, we introduce

$$(f_h, v_h)_{0,\Omega} = \sum_{K \in \mathcal{T}_h} \int_K f \Pi_{k-2}^{0,K} v_h \, dK \quad \forall v_h \in V_h; \quad (3.14)$$

Instead, for $k = 1$, we approximate f by its piecewise projection onto constants, average the test function v_h over the edges of K , and write

$$(f_h, v_h)_{0,\Omega} = \sum_{K \in \mathcal{T}_h} \left\{ |K| (\Pi_0^{0,K} f) \left(\frac{1}{N_e} \sum_{e \in \mathcal{E}^K} D_e^0(v_h) \right) \right\}. \quad (3.15)$$

3.3 The method

We propose the following nonconforming virtual element method:

$$\begin{cases} \text{find } u_h \in V_h^g(\mathcal{T}_h) \text{ such that} \\ a_h(u_h, v_h) = (f_h, v_h)_{0,\Omega} \quad \forall v_h \in V_h^0(\mathcal{T}_h). \end{cases} \quad (3.16)$$

The well posedness of method (3.16) requires further technical tools, which we derive in Section 4 below. For this reason, we postpone its proof to Theorem 4.9.

Remark 3.7. Method (3.16) is designed for meshes with rather general \mathcal{C}^1 curved edges. The assumptions on the meshes in Section 2.1, and notably the fact that curved edges are used only on the (fixed) curved boundary, will be used to derive convergence estimates in Section 6 below.

4 Stability analysis

In this section, we prove the stability bounds (3.11) for the stabilization (3.13). We proceed in some steps. First, we recall the inverse inequalities in [9, Lemma 6.3] for curved elements. The proof is independent on whether the element is curved or not.

Lemma 4.1. *Let $K \in \mathcal{T}_h$, for any $v \in H^1(K)$ such that $\Delta v \in \mathbb{P}_n(K)$, we have*

$$\|\Delta v\|_{0,K} \lesssim h_K^{-1} |v|_{1,K}.$$

We introduce the scaled norm

$$\|w\|_{\frac{1}{2},\partial K} := h_K^{-\frac{1}{2}} \|w\|_{0,\partial K} + |w|_{\frac{1}{2},\partial K},$$

and the corresponding negative norm

$$\|w\|_{-\frac{1}{2},\partial K} := \sup_{q \in H^{\frac{1}{2}}(\partial K)} \frac{\int_{\partial K} qw \, ds}{\|q\|_{\frac{1}{2},\partial K}}.$$

We recall the Neumann trace inequality for Lipschitz domains; see, e.g., [30, Theorem A.33].

Lemma 4.2. *Given an element K and v in $H^1(K)$ such that Δv belongs to $L^2(K)$, we have*

$$\|\mathbf{n}_K \cdot \nabla v\|_{-\frac{1}{2},\partial K} \lesssim |v|_{1,K} + h_K \|\Delta v\|_{0,K}.$$

Next, we state a polynomial inverse inequality on the boundary of an element K .

Lemma 4.3. *Given an element K and v_h in $V_h(K)$, we have*

$$\|\mathbf{n}_K \cdot \nabla v_h\|_{0,\partial K} \lesssim h_K^{-\frac{1}{2}} \|\mathbf{n}_K \cdot \nabla v_h\|_{-\frac{1}{2},\partial K}.$$

Proof. Using that v_h belongs to $V_h(K)$, we have that $\mathbf{n}_K \cdot \nabla v_h$ belongs to $\widetilde{\mathbb{P}}_{k-1}(e)$. So, proving the assertion boils down to proving a mapped polynomial inverse estimate; see, e.g., [4, Lemma 2.3]. The uniformity of the constant follows from the regularity of the parametrization of the curved edge. \square

We are ready to show the continuity of the stabilization $S^K(\cdot, \cdot)$ in (3.12).

Proposition 4.4. *Given an element K , v_h and w_h in $V_h(K)$, and $S^K(\cdot, \cdot)$ as in (3.12), we have the continuity property*

$$S^K(v_h, w_h) \lesssim (h_K^{-2} \|v_h\|_{0,K}^2 + |v_h|_{1,K}^2)^{\frac{1}{2}} (h_K^{-2} \|w_h\|_{0,K}^2 + |w_h|_{1,K}^2)^{\frac{1}{2}}.$$

If v_h and w_h have zero average on K or ∂K , we further deduce

$$S^K(v_h, w_h) \lesssim |v_h|_{1,K} |w_h|_{1,K}.$$

Proof. By the standard Cauchy-Schwarz inequality, it is sufficient to prove that

$$\begin{aligned} S^K(v_h, v_h) &= \sum_{e \in \mathcal{E}^K} \sum_{i=1}^k \mathbf{D}_e^i(v_h)^2 + \sum_{i=1}^{k(k-1)/2} \mathbf{D}_e^j(v_h)^2 \\ &\lesssim h_K^{-2} \|v_h\|_{0,K}^2 + |v_h|_{1,K}^2 \quad \forall v_h, w_h \in V_h(K). \end{aligned} \quad (4.1)$$

We bound the edge and boundary contributions on the left-hand side separately. We start with the first one. The standard trace inequality asserts that

$$h_K^{-1} \|v_h\|_{\partial K}^2 \lesssim h_K^{-2} \|v_h\|_{0,K}^2 + |v_h|_{1,K}^2.$$

Recall that m_i in $\mathcal{M}_{k-1}(I_e)$ are shifted and scaled monomials of maximum degree $k-1$ over I_e . Then, using the regularity of the element, we have $\|m_i\|_{I_e}^2 \lesssim h_{I_e} \approx h_e \approx h_K$. Recalling that each element has a uniformly bounded number of edges, it follows that

$$\begin{aligned} \sum_{e \in \mathcal{E}^K} \sum_{i=1}^k \mathbf{D}_e^i(v_h)^2 &= \sum_{e \in \mathcal{E}^K} |e|^{-2} \sum_{i=1}^k \left(\int_e v_h \tilde{m}_i \, ds \right)^2 \\ &\leq \sum_{e \in \mathcal{E}^K} |e|^{-2} \sum_{i=1}^k \|v_h\|_{0,e}^2 \|\tilde{m}_i\|_{0,e}^2 \lesssim \sum_{e \in \mathcal{E}^K} |e|^{-2} \|v_h\|_{0,e}^2 \sum_{i=1}^k \|m_i\|_{0,I_e}^2 \\ &\lesssim \sum_{e \in \mathcal{E}^K} |e|^{-1} \|v_h\|_{0,e}^2 \lesssim h_K^{-1} \|v_h\|_{0,\partial K}^2 \lesssim h_K^{-2} \|v_h\|_{0,K}^2 + |v_h|_{1,K}^2, \end{aligned}$$

which is the bound on the edge contributions of the stabilization in (3.12).

Next, we show the upper bound for the second term on the left-hand side of (4.1). Since we have that $\|m_j\|_{L^\infty(K)} \leq 1$ for any shifted and scaled monomial m_j in $\mathcal{M}_{k-2}(K)$, it is possible to infer

$$\begin{aligned} \sum_{j=1}^{k(k-1)/2} \mathbf{D}_e^j(v_h)^2 &= |e|^{-2} \sum_{j=1}^{k(k-1)/2} \left(\int_K v_h m_j \, dK \right)^2 \\ &\leq |e|^{-2} \sum_{j=1}^{k(k-1)/2} \left(\int_K v_h \, dK \right)^2 \leq |e|^{-1} \sum_{j=1}^{k(k-1)/2} \|v_h\|_{0,K}^2 \lesssim h_K^{-2} \|v_h\|_{0,K}^2, \end{aligned}$$

which concludes the main part of the proof. The final assertion follows immediately from known Poincaré-type inequalities on Lipschitz domains. \square

In order to show the coercivity of the stabilization $S^K(\cdot, \cdot)$ in (3.12), we need a further technical result; see, e.g., [19, Lemma 4.1] for the straight edge case (the extension to curved edges follows with a mapping argument).

Lemma 4.5. *Let e an edge of K and $a := \sum_i a_{e,i} \tilde{m}_{e,i}$ belong to $\tilde{\mathbb{P}}_n(e)$ where $\tilde{m}_{e,i}$ are the shifted and scaled monomials in $\tilde{\mathcal{M}}_n(e)$, and collect the coefficients $a_{e,i}$ in the vector \mathbf{a} . Then, we have the following norm equivalence:*

$$h_e \|\mathbf{a}\|_{\ell^2}^2 \lesssim \|a\|_{0,e}^2 \lesssim h_e \|\mathbf{a}\|_{\ell^2}^2.$$

Let $b := \sum_j b_j m_j$ belong to $\mathbb{P}_n(K)$ where m_j are the shifted and scaled monomials in $\mathcal{M}_n(K)$, and collect the coefficients b_j in the vector \mathbf{b} . Then, we have the following norm equivalence

$$h_K^2 \|\mathbf{b}\|_{\ell^2}^2 \lesssim \|b\|_{0,K}^2 \lesssim h_K^2 \|\mathbf{b}\|_{\ell^2}^2.$$

We are now ready to show the coercivity of the stabilization $S^K(\cdot, \cdot)$ in (3.12).

Proposition 4.6. *Given an element K , v_h in $V_h(K)$, and $S^K(\cdot, \cdot)$ as in (3.12), we have the coercivity property*

$$S^K(v_h, v_h) \gtrsim |v_h|_{1,K}^2. \quad (4.2)$$

Proof. Let v_h in $V_h(K)$. An integration by parts gives

$$\begin{aligned} |v_h|_{1,K}^2 &= - \int_K \Delta v_h v_h \, dK + \int_{\partial K} (\mathbf{n}_K \cdot \partial v_h) v_h \, ds \\ &= - \int_K \Delta v_h v_h \, dK + \sum_{e \in \mathcal{E}^K} \int_e (\mathbf{n}_K \cdot \partial v_h) v_h \, ds. \end{aligned} \quad (4.3)$$

Expanding Δv_h into a shifted and scaled monomial basis, and using Lemmas 4.1 and 4.5, the first integral on the right-hand side of (4.3) can be dealt with as follows:

$$\begin{aligned} - \int_K \Delta v_h v_h \, dK &= - \sum_{j=1}^{k(k-1)/2} b_j \int_K m_j v_h \, dK = - \sum_{j=1}^{k(k-1)/2} b_j |K| \mathbf{D}_e^j(v_h) \\ &\leq |K| \|\mathbf{b}\|_{\ell^2} \left(\sum_{j=1}^{k(k-1)/2} \mathbf{D}_e^j(v_h)^2 \right)^{1/2} \leq |K| \|\mathbf{b}\|_{\ell^2} S^K(v_h, v_h)^{1/2} \\ &\lesssim h_K \|\Delta v_h\|_{0,K} S^K(v_h, v_h)^{1/2} \lesssim |v_h|_{1,K} S^K(v_h, v_h)^{1/2}. \end{aligned} \quad (4.4)$$

As for the boundary integral in (4.3), first expanding $(\mathbf{n}_K \cdot \nabla v_h)$ into the $\{\tilde{m}_{i,e}\}_{i=1}^k$ basis, then employing Lemmas 4.1, 4.3, and 4.5, we infer

$$\begin{aligned} \sum_{e \in \mathcal{E}^K} \int_e (\mathbf{n}_K \cdot \nabla v_h) v_h \, ds &= \sum_{e \in \mathcal{E}^K} \sum_{i=1}^k a_{i,e} \int_e \tilde{m}_{i,e} v_h \, ds = \sum_{e \in \mathcal{E}^K} \sum_{i=1}^k a_{i,e} |e| \mathbf{D}_e^i(v_h) \\ &\leq \sum_{e \in \mathcal{E}^K} |e| \|\mathbf{a}\|_{\ell^2} \left(\sum_{i=1}^k \mathbf{D}_e^i(v_h)^2 \right)^{1/2} \leq \sum_{e \in \mathcal{E}^K} |e| \|\mathbf{a}\|_{\ell^2} S^K(v_h, v_h)^{1/2} \\ &\lesssim \sum_{e \in \mathcal{E}^K} h_e^{\frac{1}{2}} \|\mathbf{n}_K \cdot \nabla v_h\|_{0,e} S^K(v_h, v_h)^{1/2} \lesssim h_K^{\frac{1}{2}} \|\mathbf{n}_K \cdot \nabla v_h\|_{0,\partial K} S^K(v_h, v_h)^{1/2} \\ &\lesssim \|\mathbf{n}_K \cdot \nabla v_h\|_{-\frac{1}{2},\partial K} S^K(v_h, v_h)^{1/2} \lesssim (|v_h|_{1,K} + h_K \|\Delta v_h\|_{0,K}) S^K(v_h, v_h)^{1/2} \\ &\lesssim |v_h|_{1,K} S^K(v_h, v_h)^{1/2}. \end{aligned} \quad (4.5)$$

Collecting (4.4) and (4.5) in (4.3), we obtain the bound in (4.2). \square

Consider the operator $\Pi_0^0 : H^1(K) \rightarrow \mathbb{R}$ given by

$$\Pi_0^0 v := \frac{1}{|\partial K|} \int_{\partial K} v \, ds.$$

The following scaled Poincaré inequality is valid:

$$\|v - \Pi_0^0 v\|_{0,K} \lesssim h_K |v|_{1,K}. \quad (4.6)$$

To analyze the stability properties of the local discrete bilinear form, we need the following result, which states the stability in H^1 of the operator $\tilde{\Pi}_k^{\nabla,K}$ defined in (3.8)–(3.9).

Lemma 4.7. *Given an element K and v_h in $V_h(K)$, we have*

$$|\tilde{\Pi}_k^{\nabla,K} v_h|_{1,K} \lesssim |v_h|_{1,K}. \quad (4.7)$$

Proof. Introduce $\bar{v}_h = v_h - \Pi_0^0 v_h$. By definition of $\tilde{\Pi}_k^{\nabla,K}$, we have $|\tilde{\Pi}_k^{\nabla,K} \bar{v}_h|_{1,K}^2 = |\tilde{\Pi}_k^{\nabla,K} v_h|_{1,K}^2$. Therefore, substituting $q_k = \tilde{\Pi}_k^{\nabla,K} \bar{v}_h$ in (3.8) we obtain

$$\begin{aligned} |\tilde{\Pi}_k^{\nabla,K} v_h|_{1,K}^2 &= |\tilde{\Pi}_k^{\nabla,K} \bar{v}_h|_{1,K}^2 = \\ &= - \int_K \bar{v}_h \Delta \tilde{\Pi}_k^{\nabla,K} \bar{v}_h \, dK + \sum_{e \in \mathcal{E}_s^K} \int_e \bar{v}_h (\mathbf{n}_K \cdot \nabla \tilde{\Pi}_k^{\nabla,K} \bar{v}_h) \, ds + \sum_{e \in \mathcal{E}_c^K} \int_e \bar{v}_h \tilde{\Pi}_{k-1}^{0,e} (\mathbf{n}_K \cdot \nabla \tilde{\Pi}_k^{\nabla,K} \bar{v}_h) \, ds \\ &= \int_K \nabla \bar{v}_h \cdot \nabla \tilde{\Pi}_k^{\nabla,K} \bar{v}_h \, dK - \sum_{e \in \mathcal{E}_c^K} \int_e \bar{v}_h (I - \tilde{\Pi}_{k-1}^{0,e}) (\mathbf{n}_K \cdot \nabla \tilde{\Pi}_k^{\nabla,K} \bar{v}_h) \, ds \\ &\leq |\bar{v}_h|_{1,K} |\tilde{\Pi}_k^{\nabla,K} \bar{v}_h|_{1,K} + \|\mathbf{n}_K \cdot \nabla \tilde{\Pi}_k^{\nabla,K} \bar{v}_h\|_{0,\partial K} \sum_{e \in \mathcal{E}_c^K} \|\bar{v}_h\|_{0,e}. \end{aligned}$$

Applying standard trace inequality and the scaled Poincaré inequality, we infer

$$h_K^{-\frac{1}{2}} \|\bar{v}_h\|_{0,e} \lesssim h_K^{-1} \|\bar{v}_h\|_{0,K} + |\bar{v}_h|_{1,K} \lesssim |\bar{v}_h|_{1,K}$$

and

$$h_K^{\frac{1}{2}} \|\mathbf{n}_K \cdot \nabla \tilde{\Pi}_k^{\nabla,K} \bar{v}_h\|_{0,\partial K} \lesssim |\tilde{\Pi}_k^{\nabla,K} \bar{v}_h|_{1,K} + h_K |\nabla \tilde{\Pi}_k^{\nabla,K} \bar{v}_h|_{1,K} \lesssim |\tilde{\Pi}_k^{\nabla,K} \bar{v}_h|_{1,K}.$$

Combining the three above estimate, we get the assertion:

$$|\tilde{\Pi}_k^{\nabla,K} v_h|_{1,K}^2 \lesssim |\bar{v}_h|_{1,K} |\tilde{\Pi}_k^{\nabla,K} \bar{v}_h|_{1,K} \lesssim |v_h|_{1,K} |\tilde{\Pi}_k^{\nabla,K} v_h|_{1,K}.$$

□

We conclude this section, by proving stability estimates on the local discrete bilinear form $a_h^K(\cdot, \cdot)$; stability estimates for the global discrete bilinear form $a_h(\cdot, \cdot)$ are an immediate consequence.

Proposition 4.8. *Given an element K and the discrete bilinear form $a_h^K(\cdot, \cdot)$ based on the stabilization in (3.12), we have the stability estimates*

$$|v_h|_{1,K}^2 \lesssim a_h^K(v_h, v_h) \lesssim |v_h|_{1,K}^2 \quad \forall v_h \in V_h(K).$$

Proof. We first prove the lower bound. Let $\bar{v}_h = v_h - \Pi_0^0 v_h$. Using Proposition 4.6, we have

$$a^K(v_h, v_h) = a^K(\bar{v}_h, \bar{v}_h) \lesssim S^K(\bar{v}_h, \bar{v}_h) \lesssim S^K((I - \tilde{\Pi}_k^{\nabla,K})\bar{v}_h, (I - \tilde{\Pi}_k^{\nabla,K})\bar{v}_h) + S^K(\tilde{\Pi}_k^{\nabla,K} \bar{v}_h, \tilde{\Pi}_k^{\nabla,K} \bar{v}_h).$$

Since $\tilde{\Pi}_k^{\nabla,K}$ preserves constants, we can write $(I - \tilde{\Pi}_k^{\nabla,K})\bar{v}_h = (I - \tilde{\Pi}_k^{\nabla,K})v_h$. From Proposition 4.4 applied to the second term on the right-hand side of the inequality above, we infer

$$S^K(\tilde{\Pi}_k^{\nabla,K} \bar{v}_h, \tilde{\Pi}_k^{\nabla,K} \bar{v}_h) \lesssim h_K^{-2} \|\tilde{\Pi}_k^{\nabla,K} \bar{v}_h\|_{0,K}^2 + |\tilde{\Pi}_k^{\nabla,K} \bar{v}_h|_{1,K}^2.$$

By the definition of $\tilde{\Pi}_k^{\nabla,K}$, it follows that

$$\Pi_0^0 \tilde{\Pi}_k^{\nabla,K} \bar{v}_h = \Pi_0^0 \bar{v}_h = \Pi_0^0(v_h - \Pi_0^0 v_h) = 0.$$

Using (4.6) and $|\tilde{\Pi}_k^{\nabla,K} \bar{v}_h|_{1,K}^2 = |\tilde{\Pi}_k^{\nabla,K} v_h|_{1,K}^2$, we deduce

$$S^K(\tilde{\Pi}_k^{\nabla,K} \bar{v}_h, \tilde{\Pi}_k^{\nabla,K} \bar{v}_h) \lesssim |\tilde{\Pi}_k^{\nabla,K} v_h|_{1,K}^2.$$

Combining the above inequalities yields

$$a^K(v, v) \lesssim S^K((I - \tilde{\Pi}_k^{\nabla,K})v_h, (I - \tilde{\Pi}_k^{\nabla,K})v_h) + |\tilde{\Pi}_k^{\nabla,K} v_h|_{1,K}^2 = a_h^K(v_h, v_h).$$

Next, we focus on the upper bound. Recalling that $\Pi_0^0 \tilde{\Pi}_k^{\nabla,K} v_h = \Pi_0^0 v_h$, the definition of $a_h^K(\cdot, \cdot)$ in (3.13), and inequality (4.7), we conclude the proof:

$$\begin{aligned} a_h^K(v_h, v_h) &= |\tilde{\Pi}_k^{\nabla,K} v_h|_{1,K}^2 + S^K((I - \tilde{\Pi}_k^{\nabla,K})v_h, (I - \tilde{\Pi}_k^{\nabla,K})v_h) \\ &\lesssim |v_h|_{1,K}^2 + h_K^{-2} \|(I - \tilde{\Pi}_k^{\nabla,K})v_h\|_{0,K}^2 + |(I - \tilde{\Pi}_k^{\nabla,K})v_h|_{1,K}^2 \\ &\lesssim |v_h|_{1,K}^2 + |(I - \tilde{\Pi}_k^{\nabla,K})v_h|_{1,K}^2 \lesssim |v_h|_{1,K}^2. \end{aligned}$$

□

Upon using Proposition 4.8 and the Brenner-Poincaré inequality [14], we derive the following global stability estimates and the well posedness of method (3.16).

Theorem 4.9. *Given the global discrete bilinear form $a_h(\cdot, \cdot)$ based on the local stabilizations in (3.12), we have the global stability estimates*

$$|v_h|_{1,h}^2 \lesssim a_h(v_h, v_h) \lesssim |v_h|_{1,h}^2 \quad v_h \in V_h.$$

As a consequence, method (3.16) is well posed.

5 Polynomial and virtual element approximation estimates

In this section, we introduce error estimates by means of polynomial and virtual element functions. Notably, we investigate the approximation properties of the three following approximants for sufficiently regular functions v :

- the L^2 projection v_π of v into the polynomial space $\mathbb{P}_k(K)$;
- the virtual element function v_p^K defined as the solution to

$$\begin{cases} -\Delta v_p^K = -\Pi_{k-2}^{0,K} \Delta v & \text{in } K \\ \mathbf{n}_K \cdot \nabla v_p^K = \tilde{\Pi}_{k-1}^{0,e}(\mathbf{n}_K \cdot \nabla v) - c^{\partial K} & \text{on } e \in \mathcal{E}^K \\ \int_{\partial K} (v_p^K - v) \, ds = 0, \end{cases} \quad (5.1)$$

where

$$c^{\partial K} := \begin{cases} -|\partial K|^{-1} \int_K \Delta v & \text{if } k = 1 \\ 0 & \text{if } k \geq 2; \end{cases}$$

- the DoFs interpolant v_I^K in $V_h(K)$ of v defined as

$$\begin{cases} \int_K (v_I^K - v) m \, dK = 0 & \forall m \in \mathcal{M}_{k-2}(K) \\ \int_e (v_I^K - v) \tilde{m} \, ds = 0 & \forall \tilde{m} \in \tilde{\mathcal{M}}_{k-1}(e), \quad \forall e \in \mathcal{E}^K. \end{cases} \quad (5.2)$$

The functions v_π and v_I^K are well defined by construction. Also v_p^K is well defined; in fact, problem (5.1) is well posed as compatibility conditions are valid. For $k \geq 2$,

$$\begin{aligned} \sum_{e \in \mathcal{E}^K} \int_e \mathbf{n}_K \cdot \nabla v_p^K \, ds &= \sum_{e \in \mathcal{E}^K} \int_e \tilde{\Pi}_k^{0,e}(\mathbf{n}_K \cdot \nabla v) \, ds = \sum_{e \in \mathcal{E}^K} \int_e \mathbf{n}_K \cdot \nabla v \, ds \\ &= - \int_K \Delta v \, dK = - \int_K \Pi_{k-2}^{0,K} \Delta v \, dK = - \int_K \Delta v_p^K \, dK; \end{aligned}$$

for $k = 1$,

$$\begin{aligned} \sum_{e \in \mathcal{E}^K} \int_e \mathbf{n}_K \cdot \nabla v_p^K ds &= \sum_{e \in \mathcal{E}^K} \int_e \tilde{\Pi}_k^{0,e}(\mathbf{n}_K \cdot \nabla v) ds - c^{\partial K} |\partial K| = \sum_{e \in \mathcal{E}^K} \int_e \mathbf{n}_K \cdot \nabla v ds - c^{\partial K} |\partial K| \\ &= - \int_K \Delta v dK + \int_K \Delta v dK = 0 = - \int_K \Delta v_p^K dK. \end{aligned}$$

While v_p^K can be constructed elementwise providing a piecewise discontinuous virtual element approximant, the DoFs interpolant v_I^K yields a global nonconforming virtual element interpolant v_I by coupling the face DoFs. The discontinuous approximant v_p^K will be instrumental in proving the approximation properties of v_I^K .

Assumption 5.1. *Henceforth, the regularity parameter η of the curved boundary introduced in Section 1 satisfies $\eta \geq k$.*

Polynomial error estimates for v_π are well know; see e.g.[15]:

$$\|v - v_\pi\|_{0,K} + h_K |v - v_\pi|_{1,K} \lesssim h_K^{k+1} |v|_{k+1,K} \quad \forall v \in H^{k+1}(K).$$

To prove interpolation error estimates, we present an auxiliary error estimate, which can be proven proceeding along the same lines as in [10, Lemma 3.2] for the operator $\tilde{\Pi}_n^{0,e}$.

Lemma 5.2. *Let $n \in \mathbb{N}$ and the regularity parameter η of the curved boundary satisfy $\eta \geq n + 1$. Then, given an element K and any of its edges e , for all $0 \leq m \leq s \leq n + 1$, we have*

$$|v - \tilde{\Pi}_n^{0,e} v|_{m,e} \lesssim h_e^{s-m} \|v\|_{s,e} \quad \forall v \in H^s(e).$$

We also recall the properties of the Stein's extension operator E in [31, Chapter VI, Theorem 5].

Lemma 5.3. *Given a Lipschitz domain Ω in \mathbb{R}^2 and $s \in \mathbb{R}$, $s \geq 0$, there exists an extension operator $E : H^s(\Omega) \rightarrow H^s(\mathbb{R}^2)$ such that*

$$Ev|_\Omega = v \quad \text{and} \quad \|Ev\|_{s,\mathbb{R}^d} \lesssim \|v\|_{s,\Omega} \quad \forall v \in H^s(\Omega). \quad (5.3)$$

The hidden constant depends on s but not on the diameter of Ω .

We are in a position to show the first local interpolation result.

Lemma 5.4. *Given v_p^K as in (5.1), then, for all v in $H^{s+1}(K)$, $1 \leq s \leq k$, we have*

$$|v - v_p^K|_{1,h} \lesssim h^s \|v\|_{s+1,\Omega}.$$

Proof. An integration by part yields

$$\begin{aligned} |v - v_p^K|_{1,K}^2 &= -(\Delta(v - v_p^K), v - v_p^K)_{0,K} + \sum_{e \in \mathcal{E}^K} (\mathbf{n}_K \cdot \nabla(v - v_p^K), v - v_p^K)_{0,e} \\ &= -((I - \Pi_{k-2}^{0,K})\Delta v, v - v_p^K)_{0,K} + \sum_{e \in \mathcal{E}^K} ((I - \tilde{\Pi}_{k-1}^{0,e})(\mathbf{n}_K \cdot \nabla v), v - v_p^K)_{0,e} + (c^{\partial K}, v - v_p^K)_{0,\partial K} \\ &= -((I - \Pi_{k-2}^{0,K})\Delta v, v - v_p^K)_{0,K} + \sum_{e \in \mathcal{E}^K} ((I - \tilde{\Pi}_{k-1}^{0,e})(\mathbf{n}_K \cdot \nabla v), v - v_p^K)_{0,e}. \end{aligned}$$

We deduce

$$|v - v_p^K|_{1,K}^2 \leq \|(I - \Pi_{k-2}^{0,K})\Delta v\|_{0,K} \|v - v_p^K\|_{0,K} + \|v - v_p^K\|_{0,\partial K} \sum_{e \in \mathcal{E}^K} \|(I - \tilde{\Pi}_{k-1}^{0,e})(\mathbf{n}_K \cdot \nabla v)\|_{0,e}.$$

Using polynomial approximation properties and Lemma 5.2 gives

$$\|(I - \Pi_{k-2}^{0,K})\Delta v\|_{0,K} \lesssim h_K^{s-1} \|\Delta v\|_{s-1,K} \lesssim h_K^{s-1} |v|_{s+1,K}.$$

We split the edge contributions into curved and straight edges terms. As for the curved edges terms, we use Lemma (5.2) with $n = k - 1$ (recalling Assumption 5.1) and write

$$\sum_{e \in \mathcal{E}_c^K} \left\| (I - \tilde{\Pi}_{k-1}^{0,e})(\mathbf{n}_K \cdot \nabla v) \right\|_{0,e} \lesssim \sum_{e \in \mathcal{E}_c^K} h_K^{s-\frac{1}{2}} \|\mathbf{n}_K \cdot \nabla v\|_{s-\frac{1}{2},e} \lesssim h_K^{s-\frac{1}{2}} \sum_{e \in \mathcal{E}_c^K} \|\nabla v\|_{s-\frac{1}{2},e}.$$

As for the straight edges terms, since $\tilde{\Pi}_{k-1}^{0,e}$ is the standard $L^2(e)$ projection onto polynomials of maximum degree $k - 1$ over e , we use the trace inequality and write

$$\begin{aligned} \sum_{e \in \mathcal{E}_s^K} \left\| (I - \tilde{\Pi}_{k-1}^{0,e})(\mathbf{n}_K \cdot \nabla v) \right\|_{0,e} &\leq \sum_{e \in \mathcal{E}_s^K} \|\mathbf{n}_K \cdot \nabla(v - q_k)\|_{0,e} \\ &\leq \sum_{e \in \mathcal{E}_s^K} \|\nabla(v - q_k)\|_{0,e} \lesssim h_K^{-\frac{1}{2}} |v - q_k|_{1,K} + h_K^{\frac{1}{2}} |v - q_k|_{2,K} \quad \forall q_k \in \mathbb{P}_k(K). \end{aligned}$$

Standard polynomial approximation properties imply

$$\sum_{e \in \mathcal{E}_s^K} \left\| (I - \tilde{\Pi}_{k-1}^{0,e})(\mathbf{n}_K \cdot \nabla v) \right\|_{0,e} \lesssim h_K^{s-\frac{1}{2}} |v|_{s+1,K}.$$

By the Poincaré inequality and trace inequality, we infer

$$\|v - v_p^K\|_{0,K} \lesssim h_K |v - v_p^K|_{1,K}$$

and

$$\|v - v_p^K\|_{0,\partial K} \lesssim h_K^{-\frac{1}{2}} \|v - v_p^K\|_{0,K} + h_K^{\frac{1}{2}} |v - v_p^K|_{1,K} \lesssim h_K^{\frac{1}{2}} |v - v_p^K|_{1,K}.$$

Collecting the above estimates leads us to

$$|v - v_p^K|_{1,K} \lesssim h_K^s (|v|_{s+1,K} + \sum_{e \in \mathcal{E}_c^K} \|\nabla v\|_{s-\frac{1}{2},e}).$$

Summing over all the elements, we arrive at

$$|v - v_p^K|_{1,h} \lesssim h^s (|v|_{s+1,K} + \sum_{i=1}^N \|\nabla v\|_{s-\frac{1}{2},\Gamma_i}).$$

To end up with error estimates involving terms only in the domain Ω and not on its boundary, we use the Stein's extension operator of Lemma 5.3. For any curve Γ_i on the boundary of $\partial\Omega$, let \mathcal{C}_i be a domain in \mathbb{R}^2 with part of its boundary given by $\partial\mathcal{C}_i \in C^{k,1}$. Then, applying the standard trace theorem on smooth domains and the stability of the (vector valued version) Stein's extension operator in (5.3), we get

$$\|\nabla v\|_{s-\frac{1}{2},\Gamma_i} = \|E\nabla v\|_{s-\frac{1}{2},\Gamma_i} \leq \|E\nabla v\|_{s-\frac{1}{2},\partial\mathcal{C}_i} \lesssim \|E\nabla v\|_{s-\frac{1}{2},\mathcal{C}_i} \leq \|E\nabla v\|_{k,\mathbb{R}^d} \lesssim \|v\|_{s+1,\Omega}.$$

□

Thanks to the approximation properties of the piecewise discontinuous interpolant v_p^K we deduce the approximation properties of the global nonconforming interpolant v_I^K .

Lemma 5.5. *For all v in $H^{s+1}(\Omega)$, $1 \leq s \leq k$, we have*

$$|v - v_I^K|_{1,h} \lesssim h^s \|v\|_{s+1,\Omega}.$$

Proof. We follow the guidelines of [29, Proposition 3.1]. The idea is to use the definition of the DoFs interpolant so as to bound the corresponding energy error by the energy error of any piecewise discontinuous virtual element function.

Recalling the definition of v_I^K , for any v_h in $V_h(K)$, we get

$$\begin{aligned} \int_K \nabla(v - v_I^K) \cdot \nabla(v - v_I^K) &= - \int_K \Delta(v - v_I^K)(v - v_I^K) + \sum_{e \in \mathcal{E}^K} \int_e \mathbf{n}_K \cdot \nabla(v - v_I^K)(v - v_I^K) \\ &= - \int_K \Delta(v - v_h)(v - v_I^K) + \sum_{e \in \mathcal{E}^K} \int_e \mathbf{n}_K \cdot \nabla(v - v_h)(v - v_I^K) = \int_K \nabla(v - v_h) \cdot \nabla(v - v_I^K). \end{aligned}$$

The Cauchy–Schwarz inequality entails

$$|v - v_I^K|_{1,K} \leq \inf_{v_h \in V_h(K)} |v - v_h|_{1,K} \leq |v - v_p^K|_{1,K}.$$

The assertion follows summing over the elements, collecting the above inequalities, and using Lemma 5.4. \square

6 Convergence analysis

In this section, we present the error analysis in the energy and L^2 -norms for the nonconforming virtual element method (3.16); see Sections 6.1 and 6.2, respectively. In particular, we first derive Strang-like error bounds and derive optimal error estimates based on the tools in Section 5.

6.1 Convergence analysis in the energy norm

We prove the error estimates in the energy norm in some steps. First, we discuss details on geometrical errors due to the presence of curved elements.

Given a curved edge e , we denote the straight segment with endpoints given by the vertices of e by \hat{e} ; see Figure 6.1.

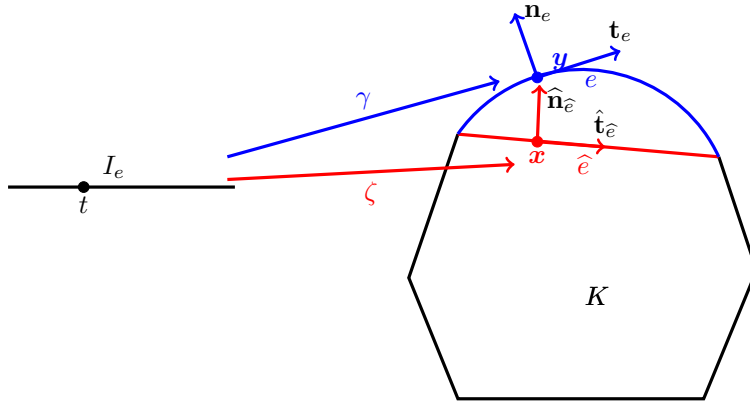


Figure 6.1: Parametrizations of the curved edge e and straight segment \hat{e} by means of the parametrizations γ and ζ .

Recall that \mathbf{n}_e is an assigned unit normal vector to the curved edge e ; fix a unit normal vector $\hat{\mathbf{n}}_{\hat{e}}$ to the segment \hat{e} . Given γ from the interval $I_e := [t_e^1, t_e^2]$ into \mathbb{R}^2 the usual parametrization of the edge e , we have the following standard estimate; see, e.g., [18, eq. (2.18)]:

$$\|\mathbf{n}_e - \hat{\mathbf{n}}_{\hat{e}}\|_{L^\infty(e)} \lesssim h_K \|\gamma\|_{W^{1,\infty}(I_e)}. \quad (6.1)$$

With the notation as in Figure 6.1, for any curved edge e with endpoints \mathbf{x}_e^1 and \mathbf{x}_e^2 , we introduce the linear map $\zeta : I_e \rightarrow \hat{e}$ given by

$$\zeta(t) = \frac{t - t_e^1}{t_e^2 - t_e^1}(\mathbf{x}_e^2 - \mathbf{x}_e^1) + \mathbf{x}_e^1.$$

We further define the constant tangent vector to \hat{e}

$$\hat{\mathbf{t}}_{\hat{e}} = \frac{\mathbf{x}_e^2 - \mathbf{x}_e^1}{t_e^2 - t_e^1}.$$

We have that $\hat{\mathbf{t}}_{\hat{e}}$ is equivalently defined as $\zeta'(t)$. Analogously, we can define $\mathbf{t}_e := \gamma'(t)$. Since we are approximating a curved edge by a straight segment, it is known that, see, e.g., [18, eq. (2.18)],

$$\|\hat{\mathbf{t}}_{\hat{e}} - \mathbf{t}_e\|_{L^\infty(I_e)} \lesssim h_K \|\gamma\|_{W^{1,\infty}(I_e)}.$$

We rewrite the two parametrizations ζ and γ as (for any $t \in I_e$)

$$\mathbf{x}(t) = \zeta(t) = \int_{t_e^1}^t \hat{\mathbf{t}}_{\hat{e}} ds + \mathbf{x}_e^1, \quad \mathbf{y}(t) = \gamma(t) = \int_{t_e^1}^t \mathbf{t}_e(s) ds + \mathbf{x}_e^1.$$

Using that the length of the reference interval is approximately h_K , the difference of the two can be estimated as follows:

$$\|\mathbf{x}(t) - \mathbf{y}(t)\| \leq \int_{t_e^1}^t \|\mathbf{t}_e(s) - \hat{\mathbf{t}}_{\hat{e}}\| ds \lesssim h_K^2. \quad (6.2)$$

Finally, we clearly have $\psi \circ \zeta \in \mathbb{P}_n(I_e)$ for any ψ in $\mathbb{P}_n(\hat{e})$. Thus, we write

$$\tilde{\psi} = \psi \circ \zeta \circ \gamma^{-1} \in \tilde{\mathbb{P}}_n(e). \quad (6.3)$$

We further introduce the H^1 projection $\Pi_k^{\nabla,K} : H^1(K) \rightarrow \mathbb{P}_k(K)$ for all elements K as follows: given a polynomial degree k ,

$$\begin{cases} \int_K \nabla q_k \cdot \nabla(v - \Pi_k^{\nabla,K} v) = 0 \\ \int_{\partial K} (v - \Pi_k^{\nabla,K} v) \end{cases} \quad \forall q_k \in \mathbb{P}_k(K), \quad \forall v \in H^1(K). \quad (6.4)$$

With this notation at hand, we derive error estimates for the Ritz-Galerkin projector $\tilde{\Pi}_k^{\nabla,K}$ defined in (3.8)–(3.9).

Lemma 6.1. *For all v in $H^{s+1}(\Omega)$, $1 \leq s \leq k$, we have*

$$|v - \tilde{\Pi}_k^{\nabla,K} v|_{1,h} \lesssim h^s \|v\|_{s+1,\Omega}. \quad (6.5)$$

Proof. According to the triangle inequality and the approximation properties of $\Pi_k^{\nabla,K}$, we have

$$|v - \tilde{\Pi}_k^{\nabla,K} v|_{1,K} \leq |v - \Pi_k^{\nabla,K} v|_{1,K} + |\Pi_k^{\nabla,K} v - \tilde{\Pi}_k^{\nabla,K} v|_{1,K} \lesssim h_K^s |v|_{s+1,K} + |\Pi_k^{\nabla,K} v - \tilde{\Pi}_k^{\nabla,K} v|_{1,K}.$$

By definition of $\tilde{\Pi}_k^{\nabla,K}$ and $\Pi_k^{\nabla,K}$, for all q_k in $\mathbb{P}_k(K)$, we can write

$$\begin{aligned} \int_K \nabla q_k \cdot \nabla(\Pi_k^{\nabla,K} v - \tilde{\Pi}_k^{\nabla,K} v) dK &= \int_K \nabla q_k \cdot \nabla v dK + \int_K \Delta q_k v dK - \sum_{e \in \mathcal{E}^K} \int_e \tilde{\Pi}_{k-1}^{0,e}(\mathbf{n}_K \cdot \nabla q_k) v ds \\ &= \sum_{e \in \mathcal{E}^K} \int_e (I - \tilde{\Pi}_{k-1}^{0,e})(\mathbf{n}_K \cdot \nabla q_k) v ds = \sum_{e \in \mathcal{E}_c^K} \int_e (I - \tilde{\Pi}_{k-1}^{0,e})(\mathbf{n}_K \cdot \nabla q_k) v ds. \end{aligned}$$

If $k = 1$, we have by definition of $V_h(K)$ that $\Pi_k^{\nabla,K} v = \tilde{\Pi}_k^{\nabla,K} v$ and the right-hand side vanishes. So, we focus on the case $k \geq 2$. We set

$$\boldsymbol{\psi} := \nabla(\Pi_k^{\nabla,K} v - \tilde{\Pi}_k^{\nabla,K} v) \in [\mathbb{P}_{k-1}(K)]^2.$$

We rewrite the above identities for the choice $q_k = \Pi_k^{\nabla, K} v - \tilde{\Pi}_k^{\nabla, K} v$ and obtain

$$\begin{aligned}
|\Pi_k^{\nabla, K} v - \tilde{\Pi}_k^{\nabla, K} v|_{1, K}^2 &= \sum_{e \in \mathcal{E}_c^K} \int_e (I - \tilde{\Pi}_{k-1}^{0, e})(\boldsymbol{\psi} \cdot \mathbf{n}_K) v \, ds \\
&= \sum_{e \in \mathcal{E}_c^K} \int_e (I - \tilde{\Pi}_{k-1}^{0, e})(\boldsymbol{\psi} \cdot \mathbf{n}_K) (I - \tilde{\Pi}_{k-1}^{0, e}) v \, ds \\
&\leq \sum_{e \in \mathcal{E}_c^K} \|(I - \tilde{\Pi}_{k-1}^{0, e})(\boldsymbol{\psi} \cdot \mathbf{n}_K)\|_{0, e} \|(I - \tilde{\Pi}_{k-1}^{0, e}) v\|_{0, e}.
\end{aligned} \tag{6.6}$$

Let $\tilde{\boldsymbol{\psi}} : e \rightarrow \mathbb{R}^2$ be the mapped polynomial associated to $\boldsymbol{\psi}|_e$, i.e., $\tilde{\boldsymbol{\psi}} := \boldsymbol{\psi} \circ \zeta \circ \gamma^{-1} \in \tilde{\mathbb{P}}_{k-1}(e)$. Since, by the same observation in (6.3), $\tilde{\boldsymbol{\psi}} \cdot \hat{\mathbf{n}} \in \tilde{\mathbb{P}}_{k-1}(e)$, we deduce

$$\begin{aligned}
\|(I - \tilde{\Pi}_{k-1}^{0, e})(\boldsymbol{\psi} \cdot \mathbf{n}_K)\|_{0, e} &\leq \|\boldsymbol{\psi} \cdot \mathbf{n}_K - \tilde{\boldsymbol{\psi}} \cdot \hat{\mathbf{n}}\|_{0, e} + \|\tilde{\Pi}_{k-1}^{0, e}(\boldsymbol{\psi} \cdot \mathbf{n}_K) - \tilde{\boldsymbol{\psi}} \cdot \hat{\mathbf{n}}\|_{0, e} \\
&\leq \|\boldsymbol{\psi} \cdot \mathbf{n}_K - \tilde{\boldsymbol{\psi}} \cdot \hat{\mathbf{n}}\|_{0, e} + \|\tilde{\Pi}_{k-1}^{0, e}(\boldsymbol{\psi} \cdot \mathbf{n}_K - \tilde{\boldsymbol{\psi}} \cdot \hat{\mathbf{n}})\|_{0, e} \leq 2\|\boldsymbol{\psi} \cdot \mathbf{n}_K - \tilde{\boldsymbol{\psi}} \cdot \hat{\mathbf{n}}\|_{0, e} \\
&\lesssim h_e^{\frac{1}{2}} \max_{\mathbf{y} \in e} |\boldsymbol{\psi}(\mathbf{y}) \cdot \mathbf{n}(\mathbf{y}) - \tilde{\boldsymbol{\psi}}(\mathbf{y}) \cdot \hat{\mathbf{n}}| \\
&\lesssim h_e^{\frac{1}{2}} (\max_{\mathbf{y} \in e} |\tilde{\boldsymbol{\psi}}(\mathbf{y}) \cdot (\mathbf{n}(\mathbf{y}) - \hat{\mathbf{n}})| + \max_{\mathbf{y} \in e} |(\boldsymbol{\psi}(\mathbf{y}) - \tilde{\boldsymbol{\psi}}(\mathbf{y})) \cdot \mathbf{n}(\mathbf{y})|).
\end{aligned} \tag{6.7}$$

By (6.1), we have the following estimate for the first term on the right-hand side of (6.7):

$$\max_{\mathbf{y} \in e} |\tilde{\boldsymbol{\psi}}(\mathbf{y}) \cdot (\mathbf{n}(\mathbf{y}) - \hat{\mathbf{n}})| \lesssim h_K \max_{t \in I_e} |\tilde{\boldsymbol{\psi}}(\mathbf{y}(t))| \lesssim h_K \max_{t \in I_e} |\boldsymbol{\psi}(\mathbf{x}(t))| \lesssim h_K \|\boldsymbol{\psi}\|_{\infty, K}. \tag{6.8}$$

As for the second term on the right-hand side of (6.7), we use (6.2):

$$\begin{aligned}
\max_{\mathbf{y} \in e} |(\boldsymbol{\psi}(\mathbf{y}) - \tilde{\boldsymbol{\psi}}(\mathbf{y})) \cdot \mathbf{n}(\mathbf{y})| &= \max_{t \in I_e} |\boldsymbol{\psi}(\mathbf{y}(t)) - \tilde{\boldsymbol{\psi}}(\mathbf{y}(t))| \\
&= \max_{t \in I_e} |\boldsymbol{\psi}(\mathbf{y}(t)) - \boldsymbol{\psi}(\mathbf{x}(t))| \lesssim h_K^{\frac{3}{2}} \|\boldsymbol{\psi}\|_{W^{1, \infty}(K)}.
\end{aligned} \tag{6.9}$$

Collecting (6.8) and (6.9) in (6.7) and using a polynomial inverse estimate, we obtain

$$\|(I - \tilde{\Pi}_{k-1}^{0, e})(\boldsymbol{\psi} \cdot \mathbf{n}_K)\|_{0, e} \lesssim h_K^{\frac{3}{2}} \|\boldsymbol{\psi}\|_{\infty, K} + h_K^{\frac{5}{2}} \|\boldsymbol{\psi}\|_{W^{1, \infty}(K)} \lesssim h_K^{\frac{1}{2}} \|\boldsymbol{\psi}\|_{0, K}. \tag{6.10}$$

On the other hand, the trace inequality for polynomial and Lemma 5.2 with $n = k - 1$ imply

$$\|(I - \tilde{\Pi}_{k-1}^{0, e}) v\|_{0, e} \lesssim h_K^{s - \frac{1}{2}} \|v\|_{s - \frac{1}{2}, e}. \tag{6.11}$$

Collecting (6.10) and (6.11) in (6.6), we deduce

$$|v - \tilde{\Pi}_k^{\nabla, K} v|_{1, h} \lesssim h^s \left(\|v\|_{s+1, \Omega} + \sum_{i=1}^N \|v\|_{s - \frac{1}{2}, \Gamma_i} \right).$$

Recalling the Stein's extension operator E in Lemma 5.3 with stability properties as in (5.3) and proceeding along the same lines of Lemma 5.4, we obtain

$$\|v\|_{s - \frac{1}{2}, \Gamma_i} \leq \|Ev\|_{s - \frac{1}{2}, \partial C_i} \lesssim \|Ev\|_{s, C_i} \leq \|Ev\|_{s, \mathbb{R}^d} \lesssim \|v\|_{s, \Omega}.$$

The assertion follows combining the two estimates above. \square

Remark 6.2. *Lemma 6.1 plays a critical role in the optimality with respect to k of the convergence estimates detailed in Theorems 6.6 and 6.7 below. A more direct approach would not exploit that e converges to \hat{e} as $h \rightarrow 0$; the ensuing approximation estimate would either be sub-optimal (order $h^{k-1/2}$ in the H^1 norm) or require a higher order polynomial degree on curved edges in the definition of the local spaces thus leading to a more computationally expensive scheme.*

Next, we provide results that are instrumental to derive optimal convergence of the method; see Theorem 6.6. We begin by recalling the discretization error on the right-hand side; see, e.g., [5, Section 4.7].

Lemma 6.3. *Let the right-hand side f of (1.1) belong to $H^{s-1}(\Omega)$, $\ell \leq s \leq k+1$, where $\ell = 2$ if $k = 1$, $\ell = 1$ if $k \geq 2$, and the discrete right-hand side f_h be as in (3.14)–(3.15). Then, for any v_h in V_h , we have*

$$|(f - f_h, v_h)_{0,K}| \lesssim \begin{cases} h|f|_{1,\Omega}|v_h|_{1,h} & \text{for } k = 1, \\ h^s|f|_{s-1,\Omega}|v_h|_{1,h} & \text{for } k > 1. \end{cases}$$

Next, we introduce a bilinear form that will allow us to take into account the nonconformity of the method in the error analysis, namely $\mathcal{N}_h : H^{\frac{3}{2}+\varepsilon}(\Omega) \times H^{1,nc}(\mathcal{T}_h, k) \rightarrow \mathbb{R}$ defined by

$$\mathcal{N}_h(u, v_h) := \sum_{K \in \mathcal{T}_h} \int_{\partial K} (\mathbf{n}_K \cdot \nabla u) v_h \, ds = \sum_{e \in \mathcal{E}_h} \int_e \nabla u \cdot \llbracket v_h \rrbracket \, ds.$$

If u , the solution to (1.1), belongs to $H^{\frac{3}{2}+\varepsilon}(\Omega)$ and is such that Δu belongs to $L^2(K)$ for all elements K , an integration by parts implies that

$$a(u, v) = (f, v_h) + \mathcal{N}_h(u, v_h) \quad \forall v_h \in V_h \subset H^{1,nc}(\mathcal{T}_h, k). \quad (6.12)$$

In the following result, we cope with the estimate of the term related to the nonconformity of the scheme.

Lemma 6.4. *Let u , the solution to (1.1) belong to $H^{s+1}(\Omega)$, $1/2 < s \leq k$. Then, for all v_h in V_h , we have*

$$|\mathcal{N}_h(u, v_h)| \lesssim h^s \|u\|_{s+1,\Omega} |v_h|_{1,h}.$$

Proof. The proof follows along the same line as those in [3, Lemma 4.1]. We briefly report it here for the sake of completeness.

From the definitions of the space $H^{1,nc}(\mathcal{T}_h, k)$ and the operator $\tilde{\Pi}_{k-1}^{0,e}$, recalling that $\mathbb{P}_0(e) \subset \tilde{\mathbb{P}}_{k-1}(e)$, finally using the Cauchy–Schwarz inequality, we find

$$\begin{aligned} \mathcal{N}_h(u, v_h) &= \sum_{e \in \mathcal{E}_h} \int_e (\nabla u - \tilde{\Pi}_{k-1}^{0,e} \nabla u) \cdot \llbracket v_h \rrbracket \, ds = \sum_{e \in \mathcal{E}_h} \int_e (\nabla u - \tilde{\Pi}_{k-1}^{0,e} \nabla u) \cdot (\llbracket v_h \rrbracket - \llbracket \Pi_0^0 v_h \rrbracket) \, ds \\ &= \sum_{e \in \mathcal{E}_h} \|\nabla u - \tilde{\Pi}_{k-1}^{0,e} \nabla u\|_{0,e} \|\llbracket v_h \rrbracket - \llbracket \Pi_0^0 v_h \rrbracket\|_{0,e}, \end{aligned}$$

where Π_0^0 denotes as usual the L^2 projection on \mathcal{T}_h -piecewise constant functions. Using Lemma 5.2 and the Poincaré inequality, for each internal edge $e = \partial K^+ \cup \partial K^-$, we get

$$\|\nabla u - \tilde{\Pi}_{k-1}^{0,e} \nabla u\|_{0,e} \lesssim h^{s-\frac{1}{2}} \|u\|_{s+\frac{1}{2},e} \lesssim h^{s-\frac{1}{2}} \|u\|_{s+1,K^+ \cup K^-}$$

and

$$\|\llbracket v_h \rrbracket - \llbracket \Pi_0^0 v_h \rrbracket\|_{0,e} \lesssim h^{-\frac{1}{2}} \|v_h - \Pi_0^0 v_h\|_{0,K^+ \cup K^-} + h^{\frac{1}{2}} |v_h - \Pi_0^0 v_h|_{1,K^+ \cup K^-} \lesssim h^{\frac{1}{2}} |v_h|_{1,K^+ \cup K^-}.$$

An analogous estimate is valid for boundary edges. The assertion follows summing over all elements. \square

Next, we estimate from above a term measuring the lack of polynomial consistency of the proposed method, i.e., the error between the bilinear functions $a(\cdot, \cdot)$ and $a_h(\cdot, \cdot)$.

Lemma 6.5. *Let u the solution to (1.1) belong to $H^{s+1}(\Omega)$, $1 \leq s \leq k$. Then, we have*

$$|a_h(u, v_h) - a(u, v_h)| \lesssim h^s \|u\|_{s+1,\Omega} |v_h|_{1,h} \quad \forall v_h \in V_h.$$

Proof. For any element K , we have

$$\begin{aligned} a_h^K(u, v_h) - a^K(u, v_h) &= a^K(\tilde{\Pi}_k^{\nabla, K} u, \tilde{\Pi}_k^{\nabla, K} v_h) + S^K((I - \tilde{\Pi}_k^{\nabla, K})u, (I - \tilde{\Pi}_k^{\nabla, K})v_h) - a^K(u, v_h) \\ &= a^K(\tilde{\Pi}_k^{\nabla, K} u, \tilde{\Pi}_k^{\nabla, K} v_h - v_h) - a^K(u - \tilde{\Pi}_k^{\nabla, K} u, v_h) \\ &\quad + S^K((I - \tilde{\Pi}_k^{\nabla, K})u, (I - \tilde{\Pi}_k^{\nabla, K})v_h) =: I_1 + I_2 + I_3. \end{aligned}$$

As for the term I_1 , we denote $\bar{v}_h = v_h - \Pi_0^0 v_h$ and use the definition of the operator $\tilde{\Pi}_k^{\nabla, K}$, then

$$\begin{aligned} I_1 &= a^K(\tilde{\Pi}_k^{\nabla, K} u, \bar{v}_h - \tilde{\Pi}_k^{\nabla, K} \bar{v}_h) = \sum_{e \in \mathcal{E}_c^K} \int_e (I - \tilde{\Pi}_{k-1}^{0,e})(\mathbf{n}_K \cdot \nabla \tilde{\Pi}_k^{\nabla, K} u) \bar{v}_h \, ds \\ &\lesssim \|\bar{v}_h\|_{0, \partial K} \sum_{e \in \mathcal{E}_c^K} \left\| (I - \tilde{\Pi}_{k-1}^{0,e})(\mathbf{n}_K \cdot \nabla \tilde{\Pi}_k^{\nabla, K} u) \right\|_{0,e}. \end{aligned}$$

Using the approximation of the operator $\tilde{\Pi}_{k-1}^{0,e}$, the Poincaré inequality, and the trace inequality, we infer, for u_π as in (3.10), the two inequalities

$$\begin{aligned} &h_K^{\frac{1}{2}} \left\| (I - \tilde{\Pi}_{k-1}^{0,e})(\mathbf{n}_K \cdot \nabla \tilde{\Pi}_k^{\nabla, K} u) \right\|_{0,e} \\ &\lesssim h_K^{\frac{1}{2}} \left\| (I - \tilde{\Pi}_{k-1}^{0,e})(\mathbf{n}_K \cdot \nabla u_\pi) \right\|_{0,e} + h_K^{\frac{1}{2}} \left\| (I - \tilde{\Pi}_{k-1}^{0,e})(\mathbf{n}_K \cdot \nabla (\tilde{\Pi}_k^{\nabla, K} u - u_\pi)) \right\|_{0,e} \\ &\lesssim h_K^s \|\mathbf{n}_K \cdot \nabla u_\pi\|_{s-\frac{1}{2}, e} + h_K^{\frac{1}{2}} \left\| \mathbf{n}_K \cdot \nabla (\tilde{\Pi}_k^{\nabla, K} u - u_\pi) \right\|_{0,e} \\ &\lesssim h_K^s \|\nabla u_\pi\|_{s-\frac{1}{2}, e} + h_K^{\frac{1}{2}} \|\nabla (u_\pi - \tilde{\Pi}_k^{\nabla, K} u)\|_{0,e} \lesssim h_K^s \|u_\pi\|_{s+1, K} + |u_\pi - \tilde{\Pi}_k^{\nabla, K} u|_{1, K} \\ &\lesssim h_K^s \|u\|_{s+1, K} + h_K^s \|u - u_\pi\|_{s+1, K} + |u_\pi - u|_{1, K} + \left| u - \tilde{\Pi}_k^{\nabla, K} u \right|_{1, K} \\ &\lesssim h_K^s \|u\|_{s+1, K} + \left| u - \tilde{\Pi}_k^{\nabla, K} u \right|_{1, K} \end{aligned} \tag{6.13}$$

and

$$h_K^{-\frac{1}{2}} \|\bar{v}_h\|_{0, \partial K} \lesssim h_K^{-1} \|\bar{v}_h\|_{0, K} + |\bar{v}_h|_{1, K} \lesssim |v_h|_{1, K}.$$

As for the term I_2 , by the continuity (4.7) and approximation properties (6.5) of $\tilde{\Pi}_k^{\nabla, K}$, we deduce

$$I_2 \leq \left| u - \tilde{\Pi}_k^{\nabla, K} u \right|_{1, K} |v_h|_{1, K}.$$

We handle the term I_3 using Proposition 4.4, the Poincaré inequality, the approximation properties (6.5) of $\tilde{\Pi}_k^{\nabla, K}$, and Lemma 4.7:

$$\begin{aligned} I_3 &\lesssim (h_K^{-2} \|(I - \tilde{\Pi}_k^{\nabla, K})u\|_{0, K}^2 + \left| (I - \tilde{\Pi}_k^{\nabla, K})u \right|_{1, K}^2)^{\frac{1}{2}} \\ &\quad (h_K^{-2} \|(I - \tilde{\Pi}_k^{\nabla, K})v_h\|_{0, K}^2 + \left| (I - \tilde{\Pi}_k^{\nabla, K})v_h \right|_{1, K}^2)^{\frac{1}{2}} \\ &\lesssim \left| (I - \tilde{\Pi}_k^{\nabla, K})u \right|_{1, K} \left| (I - \tilde{\Pi}_k^{\nabla, K})v_h \right|_{1, K} \lesssim |u - \tilde{\Pi}_k^{\nabla, K} u|_{1, K} |v_h|_{1, K}. \end{aligned}$$

The assertion follows collecting the above estimates, summing over the elements, and using the approximation properties of $\tilde{\Pi}_k^{\nabla, K}$ in Lemma 6.1. \square

We are now in a position to state the abstract error analysis in the energy norm for method (3.16) and deduce optimal error estimates.

Theorem 6.6. *Let u and u_h be the solutions to (1.1) and (3.16), respectively. Then, for every u_I in V_h , we have*

$$|u - u_h|_{1, h} \lesssim |u - u_I|_{1, h} + \sup_{v_h \in V_h} \left(\frac{|(f - f_h, v_h)_{0, \Omega}|}{|v_h|_{1, h}} + \frac{\mathcal{N}_h(u, v_h)}{|v_h|_{1, h}} + \frac{|a_h(u, v_h) - a(u, v_h)|}{|v_h|_{1, h}} \right). \tag{6.14}$$

Furthermore, if $u \in H^{s+1}(\Omega)$ and $f \in H^{s-1}(\Omega)$, with $1 \leq s \leq k$, we also have

$$|u - u_h|_{1,h} \lesssim h^s (\|u\|_{s+1,\Omega} + |f|_{s-1,\Omega}). \quad (6.15)$$

Proof. We first prove the Strang-type estimate (6.14). We split $u - u_h$ as $(u - u_I) + (u_I - u_h)$, use the triangle inequality, and get

$$|u - u_h|_{1,h} \leq |u - u_I|_{1,h} + |u_I - u_h|_{1,h}.$$

Set $e_h := u_h - u_I$. Following the lines of [3, Theorem 4.3] and recalling (6.12), the coercivity of $a_h(\cdot, \cdot)$ allows us to write

$$\begin{aligned} |e_h|_{1,h}^2 &\lesssim a_h(e_h, e_h) = a_h(u_h, e_h) - a_h(u_I, e_h) \\ &= (f_h - f, e_h)_{0,\Omega} - \mathcal{N}_h(u, e_h) - \sum_{K \in \mathcal{T}_h} a_h^K(u_I - u, e_h) - \sum_{K \in \mathcal{T}_h} a_h^K(u, e_h) + \sum_{K \in \mathcal{T}_h} a^K(u, e_h). \end{aligned}$$

The proof of (6.14) follows by standard manipulations of the right-hand side above. The error estimates (6.15) finally follow bounding the terms on the right-hand side of (6.14) by means of Lemmas 5.5, 6.3, 6.4, and 6.5. \square

6.2 Convergence analysis in a weaker norm

In this section, we prove L^2 error estimates for (3.16) based on extra assumptions on Ω . Also in this case, we follow the guidelines of the nonconforming element method error analysis; see [3, Section 4.1]. We focus on the case $k \geq 3$, and discuss the cases $k = 1$ and 2 in Remark 6.8 below.

Theorem 6.7. *Let $k \geq 3$. Assume that u and f , the solution and right-hand side of (1.1), belong to $H^{s+1}(\Omega)$, and $H^{s-1}(\Omega)$, $1 \leq s \leq k$. Let u_h be the solution to (3.16). If Ω is convex, then we have*

$$\|u - u_h\|_{0,\Omega} \lesssim h^{s+1} (\|u\|_{s+1,\Omega} + |f|_{s-1,\Omega}).$$

Proof. Consider the dual problem

$$\begin{cases} -\Delta \phi = u - u_h & \text{in } \Omega, \\ \phi = 0 & \text{on } \partial\Omega. \end{cases}$$

The convexity of Ω entails that $\phi \in H^2(\Omega) \cap H_0^1(\Omega)$ is the unique solution to the above problem and satisfies the elliptic regularity estimates

$$\|\phi\|_{2,\Omega} \lesssim \|u - u_h\|_{0,\Omega}.$$

Proceeding as in [3, Theorem 4.5] using that $k \geq 3$, and taking ϕ_I in V_h as the DoFs interpolant of ϕ in (5.2), we obtain

$$\begin{aligned} \|u - u_h\|_{0,\Omega}^2 &= \sum_{K \in \mathcal{T}_h} a^K(\phi - \phi_I, u - u_h) + \mathcal{N}_h(\phi, u - u_h) + \mathcal{N}_h(u, \phi_I) \\ &\quad + (f - f_h, \phi_I)_{0,\Omega} + \sum_{K \in \mathcal{T}_h} (a_h^K(u_h, \phi_I) - a^K(u_h, \phi_I)) \\ &\lesssim (h|u - u_h|_{1,h} + h^{s+1}) \|u\|_{s+1,\Omega} \|u - u_h\|_{0,\Omega} \\ &\quad + h^2 \|f - f_h\|_{0,\Omega} \|u - u_h\|_{0,\Omega} + \sum_{K \in \mathcal{T}_h} (a_h^K(u_h, \phi_I) - a^K(u_h, \phi_I)). \end{aligned}$$

For any element K , we have

$$\begin{aligned}
& a_h^K(u_h, \phi_I) - a^K(u_h, \phi_I) \\
&= a^K(\tilde{\Pi}_k^{\nabla, K} u_h, \tilde{\Pi}_k^{\nabla, K} \phi_I) - a^K(u_h, \phi_I) + S^K((I - \tilde{\Pi}_k^{\nabla, K})u_h, (I - \tilde{\Pi}_k^{\nabla, K})\phi_I) \\
&= a^K(\tilde{\Pi}_k^{\nabla, K} u_h, \tilde{\Pi}_k^{\nabla, K} \phi_I - \phi_I) - a^K(u_h - \tilde{\Pi}_k^{\nabla, K} u_h, \tilde{\Pi}_k^{\nabla, K} \phi_I) \\
&\quad - a^K(u_h - \tilde{\Pi}_k^{\nabla, K} u_h, \phi_I - \tilde{\Pi}_k^{\nabla, K} \phi_I) + S^K((I - \tilde{\Pi}_k^{\nabla, K})u_h, (I - \tilde{\Pi}_k^{\nabla, K})\phi_I) =: I_1 + I_2 + I_3 + I_4.
\end{aligned}$$

As for the term I_1 , we use the definition of $\tilde{\Pi}_k^{\nabla, K}$, see (3.8)–(3.9), and obtain

$$\begin{aligned}
I_1 &= \sum_{K \in \mathcal{T}_h} \sum_{e \in \mathcal{E}_c^K} \int_e (I - \tilde{\Pi}_{k-1}^{0,e})(\mathbf{n}_K \cdot \nabla \tilde{\Pi}_k^{\nabla, K} u_h) \phi_I \, ds \\
&= \sum_{K \in \mathcal{T}_h} \sum_{e \in \mathcal{E}_c^K} \int_e (I - \tilde{\Pi}_{k-1}^{0,e})(\mathbf{n}_K \cdot \nabla \tilde{\Pi}_k^{\nabla, K} u_h) (I - \tilde{\Pi}_{k-1}^{0,e}) \phi_I \, ds \\
&\leq \sum_{K \in \mathcal{T}_h} \sum_{e \in \mathcal{E}_c^K} \left\| (I - \tilde{\Pi}_{k-1}^{0,e})(\mathbf{n}_K \cdot \nabla \tilde{\Pi}_k^{\nabla, K} u_h) \right\|_{0,e} \left\| (I - \tilde{\Pi}_{k-1}^{0,e}) \phi_I \right\|_{0,e}.
\end{aligned}$$

Similarly with the inequality (6.13), we then infer

$$\begin{aligned}
& h_K^{\frac{1}{2}} \left\| (I - \tilde{\Pi}_{k-1}^{0,e})(\mathbf{n}_K \cdot \nabla (\tilde{\Pi}_k^{\nabla, K} u_h)) \right\|_{0,e} \\
&\leq h_K^{\frac{1}{2}} \left\| (I - \tilde{\Pi}_{k-1}^{0,e})(\mathbf{n}_K \cdot \nabla \tilde{\Pi}_k^{\nabla, K} u) \right\|_{0,e} + h_K^{\frac{1}{2}} \left\| (I - \tilde{\Pi}_{k-1}^{0,e})(\mathbf{n}_K \cdot \nabla (\tilde{\Pi}_k^{\nabla, K} u - u_h)) \right\|_{0,e} \\
&\lesssim h_K^s \|u\|_{s+1, K} + h_K^{\frac{1}{2}} \|\nabla \tilde{\Pi}_k^{\nabla, K} (u - u_h)\|_{0,e} \lesssim h_K^s \|u\|_{s+1, K} + |\tilde{\Pi}_k^{\nabla, K} (u - u_h)|_{1, K} \\
&\lesssim h_K^s \|u\|_{s+1, K} + |u - \tilde{\Pi}_k^{\nabla, K} u|_{1, K} + |\tilde{\Pi}_k^{\nabla, K} (u - u_h)|_{1, K} \\
&\lesssim h_K^s \|u\|_{s+1, K} + |u - \tilde{\Pi}_k^{\nabla, K} u|_{1, K} + |u - u_h|_{1, K},
\end{aligned}$$

and

$$\begin{aligned}
& h_K^{-\frac{1}{2}} \|(I - \tilde{\Pi}_{k-1}^{0,e})\phi_I\|_{0,e} \leq h_K^{-\frac{1}{2}} \|(I - \tilde{\Pi}_{k-1}^{0,e})(\phi_I - \phi)\|_{0,e} + h_K^{-\frac{1}{2}} \|(I - \tilde{\Pi}_{k-1}^{0,e})\phi\|_{0,e} \\
&\lesssim h_K^{-1} \|\phi_I - \phi\|_{0, K} + |\phi_I - \phi|_{1, K} + h_K \|\phi\|_{\frac{3}{2}, e} \lesssim |\phi_I - \phi|_{1, K} + h_K \|\phi\|_{\frac{3}{2}, e}.
\end{aligned}$$

As for the term I_2 , we set $\psi := \nabla \tilde{\Pi}_k^{\nabla, K} \phi_I - \nabla \phi_I$ and $\bar{u}_h := u_h - \Pi_0^0 u_h$, and arrive at

$$\begin{aligned}
I_2 &= -a^K(\bar{u}_h - \tilde{\Pi}_k^{\nabla, K} \bar{u}_h, \tilde{\Pi}_k^{\nabla, K} \phi_I) = - \sum_{e \in \mathcal{E}_c^K} \int_e (I - \tilde{\Pi}_{k-1}^{0,e})(\mathbf{n}_K \cdot \nabla \tilde{\Pi}_k^{\nabla, K} \phi_I) \bar{u}_h \, ds \\
&= - \sum_{e \in \mathcal{E}_c^K} \int_e (I - \tilde{\Pi}_{k-1}^{0,e})(\mathbf{n}_K \cdot \nabla (\tilde{\Pi}_k^{\nabla, K} \phi_I - \phi_I)) \bar{u}_h \, ds \\
&= - \sum_{e \in \mathcal{E}_c^K} \int_e (I - \tilde{\Pi}_{k-1}^{0,e})(\psi \cdot \mathbf{n}_K) (I - \tilde{\Pi}_{k-1}^{0,e}) \bar{u}_h \, ds \leq \sum_{e \in \mathcal{E}_c^K} \|(I - \tilde{\Pi}_{k-1}^{0,e})(\psi \cdot \mathbf{n}_K)\|_{0,e} \|(I - \tilde{\Pi}_{k-1}^{0,e}) \bar{u}_h\|_{0,e}.
\end{aligned}$$

Inequality (6.10) entails

$$\begin{aligned}
\|(I - \tilde{\Pi}_{k-1}^{0,e})(\psi \cdot \mathbf{n}_K)\|_{0,e} &\lesssim h_K^{\frac{1}{2}} \|\psi\|_{0, K} \\
&\lesssim h_K^{\frac{1}{2}} |\tilde{\Pi}_k^{\nabla, K} \phi_I - \phi_I|_{1, K} \lesssim h_K^{\frac{1}{2}} (|\phi - \phi_I|_{1, K} + |(I - \tilde{\Pi}_k^{\nabla, K})\phi|_{1, K})
\end{aligned}$$

and

$$\begin{aligned}
\|(I - \tilde{\Pi}_{k-1}^{0,e}) \bar{u}_h\|_{0,e} &\leq \|(I - \tilde{\Pi}_{k-1}^{0,e})(\bar{u} - \bar{u}_h)\|_{0,e} + \|(I - \tilde{\Pi}_{k-1}^{0,e}) \bar{u}\|_{0,e} \lesssim \|\bar{u} - \bar{u}_h\|_{0,e} + h_K^s \|\bar{u}\|_{s,e} \\
&\lesssim h_K^{-\frac{1}{2}} \|\bar{u} - \bar{u}_h\|_{0, K} + h_K^{\frac{1}{2}} |\bar{u} - \bar{u}_h|_{1, K} + h_K^s \|u\|_{s,e} \lesssim h_K^{\frac{1}{2}} |u - u_h|_{1, K} + h_K^s \|u\|_{s,e}.
\end{aligned}$$

Furthermore, we have

$$|I_3| \leq |u_h - \tilde{\Pi}_k^{\nabla, K} u_h|_{1,h} |\phi_I - \tilde{\Pi}_k^{\nabla, K} \phi_I|_{1,h}.$$

Finally, we bound I_4 :

$$\begin{aligned} |I_4| &\lesssim (h_K^{-2} \|(I - \tilde{\Pi}_k^{\nabla, K}) u_h\|_{0,K}^2 + \|(I - \tilde{\Pi}_k^{\nabla, K}) u_h\|_{1,K}^2)^{\frac{1}{2}} (h_K^{-2} \|(I - \tilde{\Pi}_k^{\nabla, K}) \phi_I\|_{0,K}^2 + \|(I - \tilde{\Pi}_k^{\nabla, K}) \phi_I\|_{1,K}^2)^{\frac{1}{2}} \\ &\lesssim |u_h - \tilde{\Pi}_k^{\nabla, K} u_h|_{1,K} |\phi_I - \tilde{\Pi}_k^{\nabla, K} \phi_I|_{1,K}. \end{aligned}$$

Each of the above terms can be readily estimated by adding and subtracting u , $\tilde{\Pi}_k^{\nabla, K} u$, ϕ , and $\tilde{\Pi}_k^{\nabla, K} \phi$:

$$\begin{aligned} |u_h - \tilde{\Pi}_k^{\nabla, K} u_h|_{1,K} &\lesssim |u - u_h|_{1,K} + \left| (I - \tilde{\Pi}_k^{\nabla, K}) u \right|_{1,K} + |\tilde{\Pi}_k^{\nabla, K} (u - u_h)|_{1,K} \\ &\lesssim |u - u_h|_{1,K} + \left| (I - \tilde{\Pi}_k^{\nabla, K}) u \right|_{1,K} \end{aligned}$$

and

$$\begin{aligned} |\phi_I - \tilde{\Pi}_k^{\nabla, K} \phi_I|_{1,K} &\lesssim |\phi - \phi_I|_{1,K} + \left| (I - \tilde{\Pi}_k^{\nabla, K}) \phi \right|_{1,K} + |\tilde{\Pi}_k^{\nabla, K} (\phi - \phi_I)|_{1,K} \\ &\lesssim |\phi - \phi_I|_{1,K} + \left| (I - \tilde{\Pi}_k^{\nabla, K}) \phi \right|_{1,K}. \end{aligned}$$

Combining the above estimates and using Lemmas 5.5, 6.3, 6.4, and 6.5, the assertion follows. \square

Remark 6.8. *The proof of Theorem 6.7 does not cover the cases $k = 1$ and 2, the reason being the presence of the term*

$$(f - f_h, \phi_I)_{0,\Omega}.$$

Following [6, Section 2.7], one can derive optimal convergence in the L^2 norm for $k = 1$ and one order suboptimal convergence for $k = 2$. In this case, optimality can be recovered by either a suitable modification of the right-hand side (using better discretization of the test function in the discrete loading term) or by adapting the enhanced version of the virtual element method.

7 The 3D version of the method

In this section, we discuss the nonconforming virtual element method for 3D curved domain and why the theoretical results are an extension of their two-dimensional counterparts. Polyhedral meshes are now employed and curved faces are the parametrizations of flat polygons. The geometric assumptions **(G1)**–**(G2)** in Section 2 are still required, but are valid for K being a polyhedron. We further require

- (G3)** every face F of K (or, if the face is curved, the associated parametric polygon \widehat{F}) is star-shaped with respect to all the points of a disk radius larger than or equal to ρh_K .

The local nonconforming virtual element space on the (possibly curved) polyhedron K reads

$$V_h(K) := \left\{ v_h \in H^1(K) \mid \Delta v_h \in \mathbb{P}_{k-2}(K), \mathbf{n}_K \cdot \nabla v_h \in \widetilde{\mathbb{P}}_{k-1}(F) \forall F \subset \partial K \right\},$$

where $\widetilde{\mathbb{P}}_{k-1}(F)$ is the push forward on F of $\mathbb{P}_{k-1}(\widehat{F})$. The definition of V_h is the natural extension of its 2D counterpart. The degrees of freedom are given by scaled (possibly curved) face moments with respect to (possibly mapped) polynomials up to order $k - 1$ and scaled bulk moments up to order $k - 2$. The global nonconforming virtual element space is obtained by a nonconforming coupling of the face degrees of freedom as in the 2D case:

$$V_h(\mathcal{T}_h) := \left\{ v_h \in H^{1,nc}(\mathcal{T}_h, k) \mid v_h|_K \in V_h(K) \forall K \in \mathcal{T}_h \right\},$$

where $[[\cdot]]_F$ is the jump across the (possibly curved) face and

$$H^{1,nc}(\mathcal{T}_h, k) := \left\{ v \in H^1(\mathcal{T}_h) \mid \int_F [[v]]_F \cdot \mathbf{n}_F q \, dF, \forall q \in \widetilde{\mathbb{P}}_{k-1}(F), \forall F \subset \partial K, K \in \mathcal{T}_h \right\}.$$

No essential modifications of the 2D structure take place in 3D. This is the major advantage of using the nonconforming version of the method. The 3D version of the conforming VEM on curved domains in [10] should involve curved virtual element spaces on faces that are currently unknown.

The construction of the local and global discrete bilinear forms in Section 3.2 directly extends to the 3D case. The only difference resides in the design of the stabilizing term that requires a different scaling. It can be proved that the stabilization

$$S^K(u_h, v_h) := \sum_{l=1}^{N_{\text{dof}}(K)} h_K \mathbf{D}^l(u_h) \mathbf{D}^l(v_h) \quad \forall u_h, v_h \in V_h(K)$$

satisfies the 3D version of the estimates in (3.11). In fact, the key technical tools in stability analysis are inverse inequalities, see Lemma 4.1; the Neumann trace inequality, see Lemma 4.2; polynomial inverse inequalities on the element boundaries, see Lemma 4.3; “direct estimates” such as Poincaré-type and trace-type inequalities. All such bounds are valid also in 3D.

The abstract error analysis is dealt with similarly to the 2D case; see Theorems 6.6 and 6.7. The only minor modification is in the definition of the nonconformity term which in 3D is defined as

$$\mathcal{N}_h(u, v) := \sum_{F \in \mathcal{E}_h^3} \int_F \llbracket v \rrbracket_F \cdot \nabla u \, dF,$$

where \mathcal{E}_h^3 denotes the set of (curved) faces in the polyhedral decomposition. Thus, the proof of error estimates for the nonconforming term follows along the same lines as in the 2D case, since [3, Lemma 4.1] is valid in arbitrary space dimension.

8 Numerical experiments

In this section, we present some numerical experiments, so as to validate of Theorems 6.6 and 6.7.

Since the energy and L^2 errors are not computable, we rather consider the computable error quantities:

$$E_{H^1} := \frac{(\sum_{K \in \mathcal{T}_h} |u - \tilde{\Pi}_k^{\nabla, K} u_h|_{1, K}^2)^{\frac{1}{2}}}{|u|_{1, \Omega}}, \quad E_{L^2} := \frac{(\sum_{K \in \mathcal{T}_h} \|u - \tilde{\Pi}_k^{\nabla, K} u_h\|_{0, K}^2)^{\frac{1}{2}}}{\|u\|_{0, \Omega}}. \quad (8.1)$$

The two quantities above convergence with the same rate as the exact errors $|u - u_h|_{1, h}$ and $\|u - u_h\|_{0, \Omega}$.

In Section 8.1, we consider two test cases on domains with curved boundary; in Section 8.2, we consider a test case with an internal curved interface and curved boundary.

8.1 Curved boundary

As a first test case, we consider the domain $\Omega = \{(x, y) | x^2 + y^2 < 1\}$, see Figure 8.1 (left-panel) and the exact (analytic) solution

$$u_1(x, y) = \sin(\pi x) \cos(\pi y).$$

The function u_1 has inhomogeneous Dirichlet boundary conditions over $\partial\Omega$.

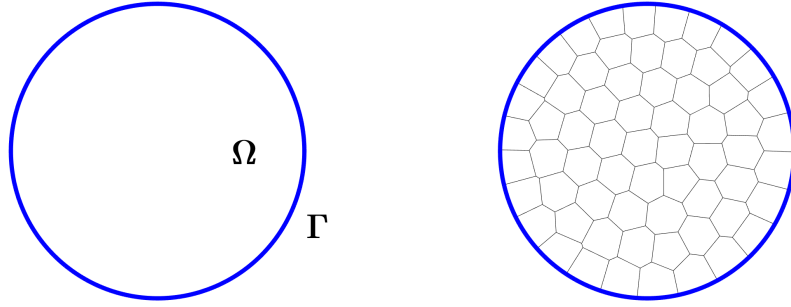


Figure 8.1: Left-panel: a circular domain Ω . Right-panel: an example of (curved) Voronoi mesh over Ω .

In Figure 8.2, we show the convergence of the two error quantities in (8.1) on the given sequence of Voronoi meshes with decreasing mesh size; see Figure 8.1 (right-panel) for a sample mesh. We consider virtual elements of “orders” $k = 2, 3,$ and 4 .

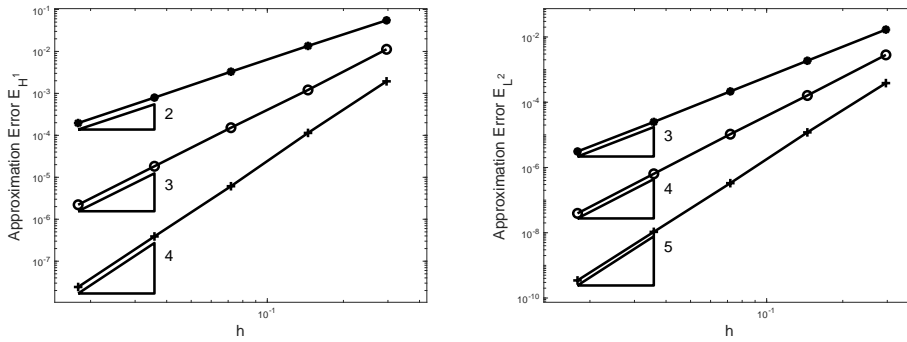


Figure 8.2: Left-panel: convergence of E_{H^1} . Right-panel: convergence of E_{L^2} . The exact solution is u_1 . Voronoi meshes with decreasing mesh size are employed. The “orders” of the virtual element spaces are $k = 2, 3,$ and 4 .

As a second test case, we consider the curved domain Ω introduced in [10] and defined as

$$\Omega := \{(x, y) \text{ s.t. } 0 < x < 1, \text{ and } g_1(x) < y < g_2(x)\}, \quad (8.2)$$

where

$$g_1(x) := \frac{1}{20} \sin(\pi x) \quad \text{and} \quad g_2(x) := 1 + \frac{1}{20} \sin(3\pi x).$$

We represent the domain in Figure 8.3. On such an Ω , we consider the exact (analytic) solution

$$u_2(x, y) = -(y - g_1(x))(y - g_2(x))(1 - x)x(3 + \sin(5x) \sin(7y)).$$

The function u_2 has homogeneous Dirichlet boundary conditions over $\partial\Omega$.

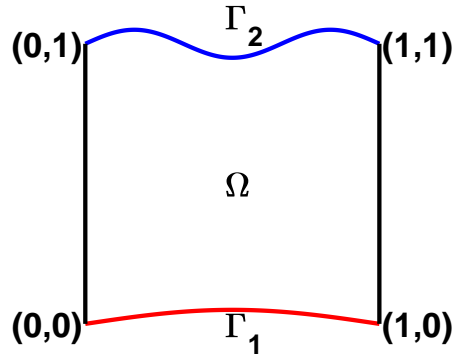


Figure 8.3: Domain Ω described in (8.2).

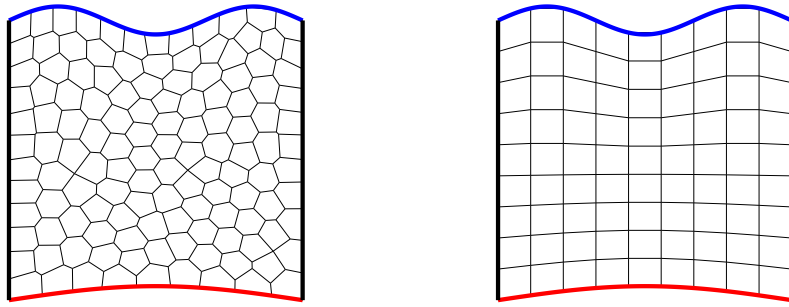


Figure 8.4: Left-panel: an example of (curved) Voronoi mesh over Ω . Right-panel: an example of (curved) quadrilateral mesh over Ω .

The finite element partition on the curved domain Ω is constructed starting from a mesh for the square $[0, 1]^2$ and mapping the nodes accordingly to the following rule:

$$(x_\Omega, y_\Omega) = \begin{cases} (x_s, y_s + g_1(x_s)(1 - 2y_s)), & \text{if } y_s \leq \frac{1}{2}, \\ (x_s, 1 - y_s + g_2(x_s)(2y_s - 1)), & \text{if } y_s \geq \frac{1}{2} \end{cases}$$

Above, (x_s, y_s) denotes the mesh generic node on the square domain $(0, 1)^2$, and (x_Ω, y_Ω) denotes the associated node in the curved domain Ω . The edges on the curved boundary consist of an arc of Γ_1 or Γ_2 , while all the internal edges are straight. In Figure 8.4, we display two examples of meshes, namely, a (curved) Voronoi and a (curved) square mesh.

In Figure 8.5, we show the convergence of the two error quantities in (8.1) on the given sequences of meshes under uniform mesh refinements for “orders” $k = 2, 3$, and 4.

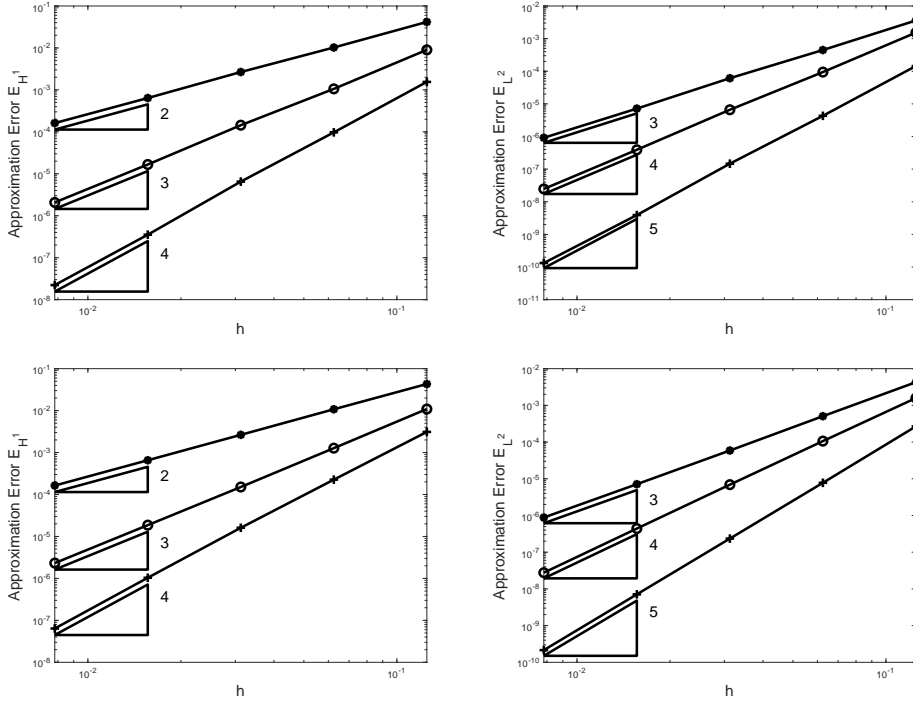


Figure 8.5: Left-panels: convergence of E_{H^1} . Right-panels: convergence of E_{L^2} . The exact solution is u_2 . We employ sequences of (curved) Voronoi meshes (first row) and (curved) square meshes (second row) with decreasing mesh size are employed. The “orders” of the virtual element spaces are $k = 2, 3$, and 4 .

The theoretical predictions of Section 6 are confirmed: convergence of order $\mathcal{O}(h^k)$ and $\mathcal{O}(h^{k+1})$ is observed for the energy and L^2 -type errors in (8.1).

Next, we approximate the curved domain by using a polygonal mesh sequence of elements with straight edges. Notably, we approximate the curved boundary by straight segments and force homogeneous Dirichlet boundary conditions; see Figure 8.6.

In Figure 8.7 we plot the results for the sequence of Voronoi meshes on the approximated domain, obtained with the standard nonconforming VEM on polygons.

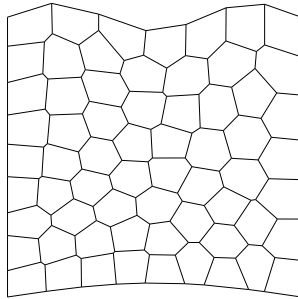


Figure 8.6: An example of (straight) Voronoi mesh over Ω .

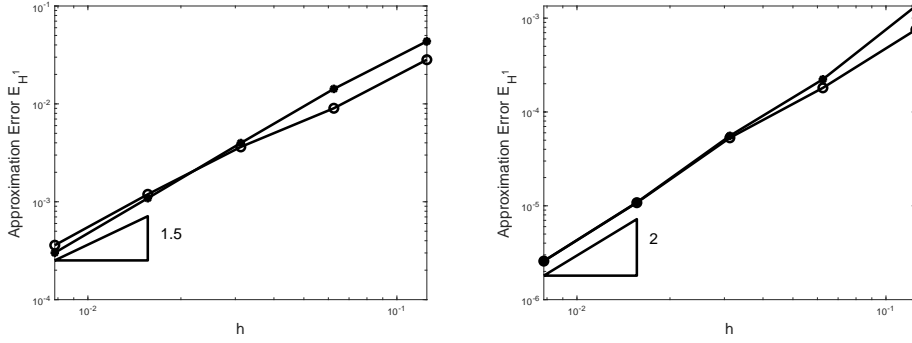


Figure 8.7: Left-panel: convergence of E_{H^1} . Right-panel: convergence of E_{L^2} . The exact solution is u_2 . Voronoi meshes with decreasing mesh size are employed. The “orders” of the virtual element spaces are $k = 2, 3$.

In this case, we observe that the geometrical error dominates and the rate of convergence is approximately 1.5 and 2 for the energy and L^2 type approximate errors in (8.1).

8.2 Curved interfaces

As a third test case, see [10], we consider the same circular domain Ω with boundary Γ_2 as in Section 8.1, and we split into two subdomains Ω_1 and Ω_2 by an internal interface Γ_1 so as Ω_2 has half the radius of Ω ; see Figure 8.8 (left-panel). Further, we are given a diffusion coefficient κ and a loading term f piecewise defined as

$$\begin{cases} \kappa = 1 & \text{in } \Omega_1, \\ \kappa = 5 & \text{in } \Omega_2, \end{cases} \quad \begin{cases} f = 5 & \text{in } \Omega_1, \\ f = 1 & \text{in } \Omega_2, \end{cases}$$

We are interested in approximating the solution u_2 to the elliptic problem

$$\begin{cases} -\operatorname{div}(\kappa \nabla u) = f & \text{in } \Omega, \\ u = 0 & \text{on } \Gamma_2, \end{cases}$$

which is given by (here $r := \sqrt{x^2 + y^2}$)

$$u_3(x, y) = u_3(r) := \begin{cases} -\frac{5}{4}r^2 + \frac{7}{20} + \frac{\ln(2)}{10} & \text{if } r \leq 1/2, \\ -\frac{1}{20}r^2 - \frac{1}{10} \ln(r) + \frac{1}{20} & \text{if } 1/2 < r < 1. \end{cases}$$

The function u_3 is analytic in Ω_1 and Ω_2 but has finite Sobolev regularity across the interface Γ_1 , see Figure 8.8).

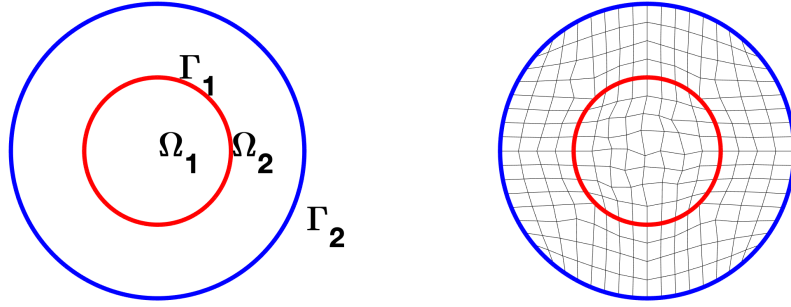


Figure 8.8: Left-panel: a circular domain Ω with a curved internal interface Γ_1 . Right-panel: an example of (curved) mesh conforming with respect to the internal interface.

In Figure 8.9, we show the convergence of the two quantities in (8.1) on the given sequence of meshes with decreasing mesh size that are conforming with respect to the curved internal interface Γ_1 ; see Figure 8.8 (right-panel). We consider virtual elements of “order” $k = 2, 3$, and 4.

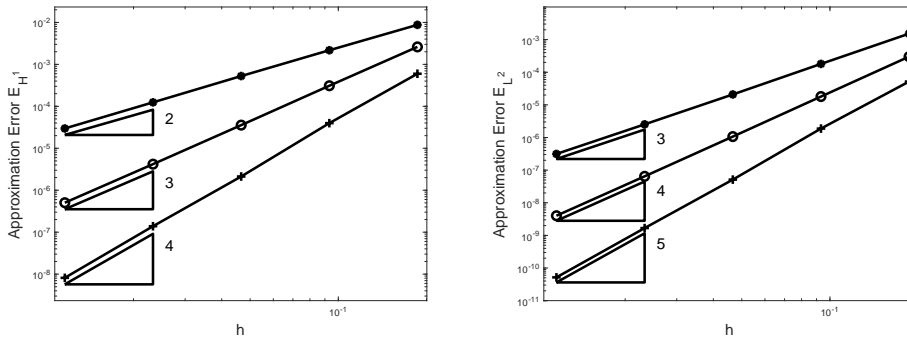


Figure 8.9: Left-panel: convergence of E_{H^1} . Right-panel: convergence of E_{L^2} . The exact solution is u_3 . Meshes with decreasing mesh size are employed that are conforming with respect to the internal interface Γ_1 . The “orders” of the virtual element spaces are $k = 2, 3$, and 4.

The theoretical predictions of Section 6 are confirmed also for domains with internal curved interface: convergence of order $\mathcal{O}(h^k)$ and $\mathcal{O}(h^{k+1})$ is observed for the energy and L^2 -type errors in (8.1).

Acknowledgment Y.L. is supported by the NSFC grant 12171244 and China Scholarship Council 202206860034. L. Beirão da Veiga was partially supported by the Italian MIUR through the PRIN Grant No. 905 201744KLJL.

References

- [1] B. Ahmad, A. Alsaedi, F. Brezzi, L. D. Marini, and A. Russo. Equivalent projectors for virtual element methods. *Comp. Math. Appl.*, 66(3):376–391, 2013.
- [2] A. Anand, J. S. Owall, S. E. Reynolds, and S. Weißer. Trefftz finite elements on curvilinear polygons. *SIAM J. Sci. Comput.*, 42(2):A1289–A1316, 2020.
- [3] B. Ayuso de Dios, K. Lipnikov, and G. Manzini. The nonconforming virtual element method. *ESAIM Math. Model. Numer. Anal.*, 50(3):879–904, 2016.

- [4] L. Beirão da Veiga and L. Mascotto. Interpolation and stability properties of low order face and edge virtual element spaces. *IMA J. Numer. Anal.*, 2022. <https://doi.org/10.1093/imanum/drac008>.
- [5] L. Beirão da Veiga, F. Brezzi, A. Cangiani, G. Manzini, L. D. Marini, and A. Russo. Basic principles of virtual element methods. *Math. Models Methods Appl. Sci.*, 23(01):199–214, 2013.
- [6] L. Beirão da Veiga, F. Brezzi, and L. D. Marini. Virtual elements for linear elasticity problems. *SIAM J. Numer. Anal.*, 51(2):794–812, 2013.
- [7] L. Beirão da Veiga, F. Brezzi, L. D. Marini, and A. Russo. The hitchhiker’s guide to the virtual element method. *Math. Models Methods Appl. Sci.*, 24(08):1541–1573, 2014.
- [8] L. Beirão da Veiga, F. Brezzi, L. D. Marini, and A. Russo. Polynomial preserving virtual elements with curved edges. *Mathematical Models and Methods in Applied Sciences*, 30(08):1555–1590, 2020.
- [9] L. Beirão da Veiga, C. Lovadina, and A. Russo. Stability analysis for the virtual element method. *Math. Models Methods Appl. Sci.*, 27(13):2557–2594, 2017.
- [10] L. Beirão da Veiga, A. Russo, and G. Vacca. The virtual element method with curved edges. *ESAIM Math. Model. Numer. Anal.*, 53(2):375–404, 2019.
- [11] S. Bertoluzza, M. Pennacchio, and D. Prada. High order VEM on curved domains. *Atti Accad. Naz. Lincei Rend. Lincei Mat. Appl.*, 30(2):391–412, 2019.
- [12] L. Botti and D.A. Di Pietro. Assessment of hybrid high-order methods on curved meshes and comparison with discontinuous Galerkin methods. *J. Comput. Phys.*, 370:58–84, 2018.
- [13] J. H. Bramble, T. Dupont, and V. Thomée. Projection methods for Dirichlet’s problem in approximating polygonal domains with boundary-value corrections. *Math. Comp.*, 26(120):869–879, 1972.
- [14] S. C. Brenner. Poincaré–Friedrichs inequalities for piecewise H^1 functions. *SIAM J. Numer. Anal.*, 41(1):306–324, 2003.
- [15] S. C. Brenner and L.R. Scott. *The mathematical theory of finite element methods*, volume 3. Springer, 2008.
- [16] E. Burman, M. Cicuttin, G. Delay, and A. Ern. An unfitted hybrid high-order method with cell agglomeration for elliptic interface problems. *SIAM J. Sci. Comput.*, 43(2):A859–A882, 2021.
- [17] E. Burman and A. Ern. A cut cell hybrid high-order method for elliptic problems with curved boundaries. In *European Conference on Numerical Mathematics and Advanced Applications*, pages 173–181. Springer, 2019.
- [18] E. Burman, P. Hansbo, and M. Larson. A cut finite element method with boundary value correction. *Math. Comp.*, 87(310):633–657, 2018.
- [19] L. Chen and J. Huang. Some error analysis on virtual element methods. *Calcolo*, 55(5):1–23, 2018.
- [20] B. Cockburn, D. A. Di Pietro, and A. Ern. Bridging the hybrid high-order and hybridizable discontinuous Galerkin methods. *ESAIM Math. Model. Numer. Anal.*, 50(3):635–650, 2016.
- [21] J. A. Cottrell, T. J. R. Hughes, and Y. Bazilevs. *Isogeometric analysis: toward integration of CAD and FEA*. John Wiley & Sons, 2009.
- [22] F. Dassi, A. Fumagalli, D. Losapio, S. Scialò, A. Scotti, and G. Vacca. The mixed virtual element method on curved edges in two dimensions. *Comput. Methods Appl. Mech. Engrg.*, 386:114098, 2021.
- [23] F. Dassi, A. Fumagalli, I. Mazzieri, A. Scotti, and G. Vacca. A virtual element method for the wave equation on curved edges in two dimensions. *J. Sci. Comput.*, 90(1):1–25, 2022.
- [24] F. Dassi, A. Fumagalli, A. Scotti, and G. Vacca. Bend 3D mixed virtual element method for Darcy problems. *Comput. Math. Appl.*, 119:1–12, 2022.
- [25] Z. Dong and A. Ern. Hybrid high-order and weak Galerkin methods for the biharmonic problem. *SIAM J. Numer. Anal.*, 60(5):2626–2656, 2022.
- [26] I. Ergatoudis, B. M. Irons, and O. C. Zienkiewicz. Curved, isoparametric, “quadrilateral” elements for finite element analysis. *Int. J. Solids Struct.*, 4(1):31–42, 1968.
- [27] C. Gürkan, E. Sala-Lardies, M. Kronbichler, and S. Fernández-Méndez. eXtended Hybridizable Discontinuous Galerkin (X-HDG) for void problems. *J. Sci. Comput.*, 66(3):1313–1333, 2016.
- [28] M. Lenoir. Optimal isoparametric finite elements and error estimates for domains involving curved boundaries. *SIAM J. Numer. Anal.*, 23(3):562–580, 1986.
- [29] L. Mascotto, I. Perugia, and A. Pichler. Non-conforming harmonic virtual element method: h - and p -versions. *J. Sci. Comput.*, 77(3):1874–1908, 2018.
- [30] C. Schwab. *p - and hp - Finite Element Methods: Theory and Applications in Solid and Fluid Mechanics*. Clarendon Press Oxford, 1998.
- [31] E. M. Stein. *Singular integrals and differentiability properties of functions*, volume 2. Princeton University Press, 1970.
- [32] G. Strang and A. E. Berger. The change in solution due to change in domain. In *Partial differential equations (Proc. Sympos. Pure Math., Vol. XXIII, Univ. California, Berkeley, Calif., 1971)*, pages 199–205. Amer. Math. Soc., Providence, R.I., 1973.
- [33] V. Thomée. Polygonal domain approximation in Dirichlet’s problem. *IMA J. Appl. Math.*, 11(1):33–44, 1973.
- [34] L. Yemm. A new approach to handle curved meshes in the hybrid high-order method. <https://arxiv.org/abs/2212.05474>, 2023.